



Published in final edited form as:

*Anal Chem.* 2016 January 5; 88(1): 354–380. doi:10.1021/acs.analchem.5b04077.

## Microfluidic Sample Preparation for Single Cell Analysis

Sanjin Hosic<sup>†</sup>, Shashi K. Murthy<sup>†,‡</sup>, and Abigail N. Koppes<sup>\*,†</sup>

<sup>†</sup>Department of Chemical Engineering, Northeastern University, Boston, MA, USA

<sup>‡</sup>Barnett Institute of Chemical and Biological Analysis, Northeastern University, Boston, MA, USA

### 1. INTRODUCTION

Single cell analysis is the measurement of transcription, translation, regulatory, and signaling events within individual cells at the molecular level. The goal is to analyze and synthesize information from single cells in order to holistically understand the cell population. This reductionist approach allows researchers to unravel how molecular events within a single cell link to the behavior of tissues, organs, and eventually whole organisms. Single cell analysis has gained significant traction over the past decade, as evidenced by the number of recent reviews.<sup>1–3</sup> The field continues to expand exponentially and necessitates a review of developments that have occurred over the past three years. The transition from bulk to single cell analyses has been fueled in part by studies highlighting single cell heterogeneity and stochasticity relative to whole cell populations.<sup>4–5</sup> The random variability in these cell populations is likely due to intrinsic noise. Intrinsic noise refers to cell-to-cell variation in transcription and translation products such as ions, mRNA, and proteins. These components are governed by phenomena such as reaction rates and molecular collisions. Given the flexible and dynamic nature of the cell membrane, reactions and molecular collisions will occur stochastically. Thus, it is unreasonable to assume that all cells within a population are equal at any given moment, and only a large number of single cell measurements will reveal this heterogeneity and provide the statistical power to model it. Modeling approaches are necessary for interpreting the massive amount of data generated with single cell analyses such as whole genome sequencing. Furthermore, these models may ultimately guide the optimum operation of a bioprocess such as the production of valuable biotherapeutics via cell culture or deterministic stem cell reprogramming for regenerative medicine.<sup>6</sup>

Single cell analysis is not only driven by stochasticity of homogeneous cell populations as in cell cultures, but also by the need to analyze tissues composed of multiple distinct cell types and the need to identify discrete subpopulations among seemingly identical cells. For example, the intestinal stem cell niche is a tissue composed of several different cell types such as stem cells, Paneth cells, Goblet cells, enterocytes, and enteroendocrine cells. Currently, researchers are investigating the existence of distinct intestinal stem cell populations. Much of the current literature supports the existence of a proliferative stem cell

\*Corresponding author. Address: Northeastern University, 360 Huntington Ave., 313 Snell Engineering, Boston, MA 02115, U.S.A; a.koppes@neu.edu.

population responsible for epithelial homeostasis and a quiescent stem cell population responsible for regeneration in response to injury.<sup>7</sup> However, conflicting reports preclude definitive stem cell biomarkers for each population.<sup>7</sup> Non-biased single cell molecular analysis may settle the debate over intestinal stem cell markers once and for all.

Such findings have driven the development of new analytical systems to probe biology at the resolution of a single cell. In order to study single cells accurately and efficiently, systems with high sensitivity and throughput are needed. The small dimensions of microfluidic systems enable single cell and reagent manipulation with minimal dilution,<sup>8</sup> resulting in high sensitivity assays. Furthermore, microfluidic systems offer several key advantages toward the study of single cells including facile automation, parallelization, and reagent reduction.<sup>8</sup> Early researchers found that sample preparation such as cell manipulation, compartmentalization, and lysis was significantly more difficult to implement at the single cell scale compared to in bulk. However, sample preparation preceding molecular analysis has also been miniaturized, allowing facile sample processing. As such, microfluidic systems have been developed and applied toward the study of single cells extensively.<sup>9-10</sup> Given microfluidics' instrumental role in single cell analysis up to this point, we can expect continued innovations in microfluidics to better enable single cell biology.

In this review, novel microfluidic techniques currently used toward sample preparation and subsequent single cell analysis are highlighted. Techniques are discussed in terms of discrete sample preparation steps that may be necessary for characterizing single cells; tissue dissociation into cell suspensions, sorting heterogeneous cell populations into homogenous populations, isolating, and lysing single cells (Figure 1). With each discrete step, conventional approaches are discussed first and then microfluidic based strategies are reviewed. Finally, the future direction for developing microfluidic single cell analysis technology is discussed.

## 2. SAMPLE PREPARATION

### A. Tissue Dissociation

**Conventional Approaches**—The first step toward single cell analysis is obtaining cells from a source. To enable inferences regarding the function of an organ or even a whole organism via single cell data, it is vital that the cells are representative of that specific organ or organism. Intact tissues obtained via biopsy are an excellent source of cells, and are representative of their native microenvironment. To obtain suspended cells from the harvested intact tissue, the extracellular matrix and cell-cell junctions holding the cells together in a 3D structure must be disrupted. Conventional methods consist of incubating the intact tissues with enzymes such as collagenase in order to digest proteins in the extracellular matrix. Exposure to chelating agents such as ethylenediaminetetraacetic acid (EDTA) binds to  $\text{Ca}^{2+}$  and disrupts the cell-to-cell adherens junctions regulated by transmembrane cadherin proteins. After chemical exposure, intact tissue is often dissociated into a cell suspension via gentle mechanical agitation such as pipetting or inversion. For example, Robin et al.<sup>11</sup> described a procedure to isolate human myogenic cells following a patient muscle tissue biopsy. The procedure called for the addition of dispase II and

collagenase D to minced tissue followed by pipetting of the mixture. The same study described a similar protocol to isolate fibroblasts from a patient skin biopsy by exposing the tissue to collagenase followed by mincing.<sup>11</sup> Many more dissociation enzymes are in use, for example: trypsin,<sup>12</sup> elastase,<sup>13</sup> and hyaluronidase<sup>14</sup> to name a few. For liquid biopsies, such as a blood draw, cell dissociation is not required. In these cases, cell sorting may be the first sample preparation step. This is common for circulating tumor cell enumeration, which is discussed in later sections.

A critical goal of any tissue dissociation protocol is to yield as many viable cells as possible for downstream workup. Several protocol parameters may affect the outcome of the tissue dissociation such as animal species, tissue type, which enzyme and or chelator is used, chemical concentration, incubation time, temperature, agitation method, etc. Parameters that can be controlled are determined empirically through trial and error to maximize the cell yield and viability. Though developing a dissociation protocol appears an arduous task, a plethora of scientific literature can serve as a starting point for isolating cells from various mammalian tissue including but not limited to: murine brain tissue,<sup>15</sup> murine, rat, and human heart tissue,<sup>16–18</sup> and murine intestine.<sup>19</sup> Much effort has been dedicated to optimizing tissue dissociation because errors upstream can propagate to the downstream cell assay, negatively impacting the data.

The enzymatic and mechanical tissue dissociation protocols described above have inherent drawbacks making these conventional protocols less than ideal. For example, isolating human adipose derived adult stem cells from tissue obtained via liposuction, rather than bone marrow, required 8–10 h of continuous labor.<sup>20</sup> In addition to being highly labor intensive, long protocols significantly increase contamination risk, operator error, and variability. Furthermore, enzymatic digestion may result in a loss of cell surface protein expression.<sup>21</sup> A loss of cell surface proteins can negatively impact the ability to sort cells via fluorescent activated cell sorting (FACS), a current workhorse in cell isolation and purification. This led to groups devising alternative schemes with shorter and or non-enzymatic workflow.<sup>21</sup> While the majority of current microfluidic research describes downstream applications, emerging microfluidic devices are addressing issues in the upstream tissue dissociation step.

**Microscale Approaches**—Traditional batch tissue culture operations rely on supplying cells with nutrients and refreshing culture medium at discrete time points, thereby creating variability in nutrient and waste product concentrations throughout the cells' life cycle. To create an environment that better mimics the flux of in vivo tissue, Hattersley et al.<sup>22</sup> developed a microfluidic device for on-chip perfusion culture, analysis, and dissociation of intact rat liver tissue (Figure 2A). On-chip tissue dissociation was performed followed by a viability assay. In brief, the immobilized tissue was perfused with ethylene glycol tetraacetic acid (EGTA) to scavenge Ca<sup>2+</sup> ions followed by Earl's balanced salt solution (EBSS) to remove EGTA, which may prevent collagenase inhibition. Next, the tissue was digested by perfusion with collagenase solution. Finally, the tissue was perfused with ice-cold dispersal buffer at a high flow rate (500  $\mu$ L/min). The cells were collected at the device output directly into a centrifuge tube to be used for cell pelleting. Following on-chip enzymatic dissociation, a Trypan blue assay indicated that 78 + 2.4 % cells were viable, comparable

with traditional dissociation methods.<sup>22</sup> While still utilizing an enzymatic mechanism, this microfluidic approach reduces the duration of cell or tissue exposure to non-sterile conditions, thereby minimizing contamination risk. However, only approximately 30,000 cells were isolated from 4 mm<sup>3</sup> of tissue via a two hour collagenase perfusion. These results indicate a low yield of total cells, potentially due to an overly gentle procedure. Additionally, a two hour dissociation procedure may be unsuitable for applications where gene expression analysis is the ultimate goal, since gene expression occurs on the same time scale.

With a similar goal of reducing foreign contamination, Wallman et al.<sup>23</sup> built a microfluidic device, termed “biogrid”. The device addressed contamination risk in addition to non-enzymatic requirements and scalability in the clinical or commercial production of neural stem cell therapies. Neural stem cells can be cultured in suspension as stem and progenitor cell aggregates called neurospheres, requiring periodic passaging and subsequent expansion.<sup>24</sup> To conform to good manufacturing practice (GMP) guidelines in a clinical or commercial setting, contamination risk should be minimized by passaging neurospheres in closed, sterile equipment without the use proteolytic enzymes. Proteolytic enzymes are biologically active molecules and therefore have the potential to introduce contamination or toxicity. Non-enzymatic methods such as mechanical means involving scalpels<sup>25</sup> are not scalable and pose a significant contamination risk due to environmental exposure or contaminated tools. The described device consisted of a 3 x 3 mm, 170 μm thick silicon chip, with a sharp edged grid in the center. The grid’s edges were 20 μm thick with 200 μm edge to edge spacing (Figure 2C). By passing a neurosphere suspension through the biogrid, neurospheres greater than the grid-to-grid spacing were mechanically dissociated while aggregates and cells smaller than the spacing were unaffected. Comparing the biogrid with traditional enzymatic protocols, the growth rate of passaged neurospheres was more reproducible. However, enzymatically passaged cultures exhibited a greater growth rate compared to biogrid passaged cultures. Cultures passaged with both methods indicated equivalent growth active fractions in passaged cultures. Grid spacing and edge width can be tailored to dissociate various cell aggregates, such as embryonic stem cell spheres, as demonstrated by Wallman et al.<sup>23</sup> Despite offering a closed, scalable, non-enzymatic method for neurosphere dissociation, strictly single cell dissociation was not achieved with aggregates remaining post processing. Single cell dissociation would be critical for optimal passaging and cell culture operation by increasing yield of the culture system. Furthermore, single cell dissociation is crucial for downstream workups such as FACS or single cell molecular analysis

To achieve strictly single cell dissociation from neurospheres, Lin et al.<sup>26</sup> designed a microfluidic cell dissociation chip, termed “μ-CDC”. The single channel device consisted of micro pillars 50 μm wide and 167 μm tall with 20 μm spacing between adjacent pillars (Figure 2B). Neurospheres of DC115 and KT98 brain tumor mouse models were dissociated into single cells by passage through the pillar array at 3–15 mL/min via a syringe pump. The yield of single cells following μ-CDC dissociation was 91–95% with single cell viabilities of 80–85%, compared to 50% achieved via trituration. However, the rate of neurosphere reformation by microfluidic dissociated cells was lower compared to enzymatically dissociated neurospheres, indicating that the induced shear stress may negatively affect cells.

Furthermore recovery of KT98 cells and DC115 cells was approximately 75% and 93%, respectively, indicating that the cell type affects device performance. The authors stated that optimizing the geometry and flow rate may potentially address recovery and neurosphere reformation for improved cell expansion.

Low cell recovery during tissue dissociation is also a concern in cell based analyses of tumor tissue, particularly for smaller and harder to obtain clinical samples, such as those obtained by fine needle aspirate biopsy. Qui et al.<sup>27</sup> designed a microfluidic device for dissociating tumor tissue equal to or less than 1 mm into single cells (Figure 2D). The device consisted of branching channels. The dissociation is performed by repeated constriction and expansion along each channel, generating shear forces during fluid flow. The device process was evaluated with cell suspensions featuring small HCT 116 colon cancer cell clusters, intact cell monolayers grown from HCT 116 cells, and tumor spheroid derived from HCT 116, LS 174T, and NCI-H1650 cancel cell lines via the hanging drop method. With respect to intact cell monolayers, non-enzymatic device dissociation achieved the same cell yields but showed a significant increase in the single cell population, from 61% to 95% when compared to a control dissociation method utilizing trypsin-EDTA, vortexing, and pipetting. With respect to tumor spheroids, a combination of device dissociation with 5 minute EDTA pretreatment resulted in an increase in single cell population from ~60% to 90% compared to dissociating tumors via vortexing and pipetting following 5 minute EDTA pretreatment. In addition to increasing single cell yield, the device dissociation protocols were completed in 10 minutes or less across all experiments and enabled non-enzymatic spheroid dissociation. However, it was noted that the model cell lines used in the study may not be representative of actual human clinical specimens. Patient samples are more complex in that they contain a heterogeneous cell population, blood vessels, and lower stromal content.<sup>28</sup> As such, patient derived tumor tissue may respond differently compared to the immortalized cell lines and remains to be tested. Nevertheless, the device provides high single cell yields, crucial for limited samples. Furthermore, the device offers rapid and non-enzymatic tissue dissociation, which is critical for measuring endogenous molecular expression.

Microfluidic tissue dissociation is still nascent when compared to other microfluidic applications, but the advantages are already clear. Performing tissue dissociation in flow offers easier scale-up and higher productivity, both necessary for commercialization. Cell and/or tissue handling is minimized by utilizing closed systems, thereby reducing contamination risk. Flow environments within laminar microfluidics can be tightly controlled, offering higher reproducibility and the dissociation mechanisms are on the size scale of cellular samples, resulting in higher single cell yields. The smaller process volumes inherent to microfluidics also allow facile and reliable dissociation of smaller and limited clinical samples. Finally, non-enzymatic methods are particularly attractive from a regulatory standpoint and allow scientists to isolate single cells that maintain endogenous surface marker expression. As such, we can expect this research field to gain significant traction in the future.

## B. Cell Sorting

**Conventional Approaches**—Bulk tissue dissociation typically results in a heterogeneous cell suspension. However, scientists are often interested in studying one target cell type within the greater tissue population; hence, the next step in single cell workflow is to sort the heterogeneous cell suspension into homogeneous fractions. The most commonly used method for sorting populations, FACS, relies on conjugating cell surface proteins specific to one cell type with an antibody coupled to a fluorescent dye. Suspended cells then flow past a laser beam, which excites the dye and a detector records several parameters including the emitted color (Figure 3A). Single cell droplets are given a specific charge based upon the fluorescent dye color and then deflected into the correct container by an electric field. Since its invention in 1969,<sup>29</sup> FACS has evolved and maintains its position as a cell enrichment workhorse capable of detecting as many as 14 fluorescent markers and sorting 50,000 cells per second.<sup>30</sup> For example, Sanchez-Freier et al.<sup>31</sup> performed cell sorting of cultured human embryonic stem cells and induced pluripotent cells to exclude partially differentiated and dead cells. Using a five laser FACS system, double-positive cells were directly sorted to each well of a 96 well plate where quantitative real-time polymerase chase reaction (qPCR) was carried out. Direct integration with well plates for single cell compartmentalization is another advantage of FACS. Nevertheless, FACS has several limitations. FACS instruments are costly, typically several hundred thousand dollars. As such, they are usually only available at core facilities, which limits widespread use to smaller research programs. Furthermore, decreased cell viability is frequently observed due to long processing times.

An alternative to FACS is the use of magnetic fields to separate cells with marker specific magnetic labels, termed magnetic activated cell sorting or MACS (Figure 3B). Since the development of magnetic-activated cell sorting (MACS) over 20 years ago, this technique has evolved considerably.<sup>32</sup> Treutlein and coworkers<sup>33</sup> used MACS to enrich distal lung epithelial cells from a heterogeneous population containing leukocytes and alveolar macrophages for single cell RNA sequencing. MACS offers cost effective cell enrichment compared to FACS and several commercial MACS systems are in existence. The FDA approved CELLSEARCH® system allows for automated staining, imaging, and enumeration of circulating tumor cells (CTCs) from a 7.5 mL blood sample. This system is useful for bulk CTC enrichment but cannot be integrated directly with well plates for single cell molecular analysis. To overcome this, Neves et al.<sup>34</sup> developed a protocol for CELLSEARCH® based CTC enrichment, FACS sorting and isolation into PCR tubes followed by single cell molecular analysis via qPCR. This study illustrated the combination of CELLSEARCH® and FACS for molecular analysis of single CTCs.

Despite wide adoption, both FACS and MACS have drawbacks that limit their widespread use or the fidelity of subsequent single cell analyses. For example, FACS machines require high technical expertise to operate and can be costly, ranging anywhere from \$100,000 to \$500,000. MACS introduces an inherent risk of sample contamination due to batch-wise processing. Both methods rely on labeling of cell surface markers to separate cells, which adds to the overall processing time and viability reduction. It has been shown that immunomagnetic labeling can alter gene expression,<sup>35</sup> motivating the development of

methods to detach magnetic beads from purified cells. These limitations have led to the development of microfluidic cell sorting platforms as detailed below.

**Microscale Approaches**—Microfluidic devices are inherently advantageous cell sorting platforms compared to conventional methodologies for a variety of reasons. Miniaturized devices allow for reduced reagent consumption and portability.<sup>8</sup> The devices can be made using standard micro fabrication tools and soft lithography,<sup>36</sup> thereby lowering production cost. Laminar fluid dynamics in devices allows for predictable spatiotemporal control of flowing cells, thereby enabling oftentimes passive and label-free cell separation. Passive sorting translates to simplified device operation and reduces the high technical expertise required for FACS. Sorting is typically accomplished continuously in an enclosed device, minimizing contamination risk. The advent of microfluidic cell sorting technology has alleviated many of the limitations imposed by FACS and MACS. However, microfluidic cell sorting requires further development in key areas if it is to displace conventional technologies. A major drawback of microfluidic systems is lower throughput compared to commercial FACS machines. Thus, this has been a major research focus and is steadily gaining traction. Finally, microfluidic devices fabricated via soft lithography are prone to cell adhesion and clogging, limiting their long term use. The body of literature regarding microfluidic enabled cell sorting is extensive and there are a number of excellent reviews of work in this area.<sup>37–41</sup> Here, we discuss select cell separation modalities that have specific relevance to single cell analysis as a step in the sample preparation sequence. Typically, knowledge of the target cell type's properties relative to the whole population guides the selection of an appropriate separation mechanism.

**Active Mechanisms**—Microfluidic cell sorting methods that rely on external force fields, such as electrical or magnetic fields, are discussed first. These force fields induce cell movement. The fields are generated by integration of specialized parts with a microfluidic chip such as electrodes or magnets. Active cell sorting methods are advantageous over passive sorting mechanisms due to increased cell control and specificity. However, fabricating microfluidic chips with specialized, integrated features is more complicated. This can limit chip fabrication to laboratories with prior experience or the ability to outsource. At the very least, chip production time may be increased. Furthermore, operation of devices with active sorting mechanisms generally requires power and control systems, thereby increasing cost. Nevertheless, a plethora of active cell sorting devices have been reported and will be described in more detail below.

**Electrophoresis and Dielectrophoresis**—Most cells typically possess a negative surface charge at neutral pH. As such, suspended cells will move toward a positive electrode under a constant electric field.<sup>42</sup> In a liquid, the cells will be directed with a velocity that can be derived from a force balance. The dominant forces acting on the cell are the Coulomb and drag forces. In order to separate different cell types, the cells must have a difference in charge or size.<sup>43</sup> This separation mode is termed electrophoresis (EP) (Figure 4A). Takahashi et al.<sup>44</sup> designed a device in which two laminar flow streams converge at the center of the device. Cells are introduced in one stream and imaged every 1/30<sup>th</sup> of a second as they pass the convergence point. A specific cell is identified via phase contrast and

fluorescence, at which point a voltage is applied to electrodes connected between the two streams. The electrophoretic force causes the cell to jump from one stream to the other. Similarly, Guo et al.<sup>45</sup> separated single cells encapsulated in an aqueous-oil droplet into different streams via a pulsed electric field. In general, publications utilizing EP to sort heterogeneous cell suspensions are few due to insignificant specificity in EP mobility among cell types.<sup>43, 46</sup>

Contrary to EP, dielectrophoresis (DEP) is used much more frequently for cell sorting because of higher specificity in dielectric properties among cell types. For example, it was shown<sup>47</sup> via dielectrophoretic field-flow fractionation (DEP-FFF) that all 60 cell types of the NCI-60 tumor cell panel, an array of human cancer cell lines, have dielectric properties different from peripheral cell types (monocytes, T-lymphocytes, basophils, neutrophils, eosinophils, B-lymphocytes, erythrocytes) and therefore could be isolated via DEP. In DEP-FFF, a heterogeneous mixture of cells is flowed through a channel while electrodes at the channel bottom generate an upward DEP force that balances the downward gravity force (Figure 4B). Each cell type stabilizes at a unique channel height, at which there is a distinct flow velocity due to a parabolic velocity profile.<sup>43</sup> For DEP, cells do not need to possess a surface charge. Instead, an alternating current typically polarizes the cell. The cell then moves toward or away from the area of highest electric field density. Thus, a spatially non-uniform electric field is required in order to impart a force on the polarized cell. The migration direction is dependent on the electrical permeability of the cell relative to the surrounding fluid. Negative dielectrophoresis (nDEP), movement away from the field maxima, results when the fluid has higher permeability. The opposite is true for positive dielectrophoresis (pDEP), movement toward the field maxima.<sup>43</sup> DEP has a few advantages compared to EP, namely; greater cell sorting specificity and the use of an alternating current prevents electrochemical reactions from occurring at the electrodes and limits detriment to cell viability.

The enumeration of rare circulating tumor cells (CTCs), cells that have shed from a primary tumor and entered the blood stream, for metastatic cancer prognosis demands CTC isolation from a dense heterogeneous cell suspension, blood.<sup>48</sup> Gascoyne et al.<sup>49</sup> utilized batch DEP-field flow fractionation (DEP-FFF) to separate CTCs from peripheral blood cells and achieved a 90% CTC recovery when a 0.5 mL sample containing approximately  $10^6$  cells/mL was applied to the device. However, this sample size represented less than 5% of clinically relevant sample sizes. Improving upon this method, Shim et al.<sup>50</sup> designed a continuous DEP-FFF device that was capable of processing  $4 \times 10^7$  peripheral blood cells in less than one hour, corresponding to a more realistic clinical sample size. Following isolation via the DEP-FFF device, the isolated cells were identified as patient derived cancer cells via a genotype array. Many other studies have reported CTC isolation from blood, focusing on increasing separation throughput, yield, and CTC purity. Moon et al.<sup>51</sup> serially combined hydrodynamic and DEP separation modalities on one chip in to enable high throughput and purity. The integrated separation resulted in label free CTC isolation at a flow-rate of 126  $\mu\text{L}/\text{min}$  with 99% and 94% removal of red and white blood cells, respectively. This approach leveraged a hydrodynamic modality to remove blood cells in high throughput and a subsequent DEP force to precisely isolate CTCs. Serial combinations



of separation modalities can be utilized to achieve multifaceted goals, high throughput and purity in this case.

Similarly, towards the goal of achieving simultaneous high throughput and multiple parameter sorting, Kim and Soh<sup>52</sup> built an integrated dielectrophoretic-magnetic activated cell sorter, and demonstrated sorting of three different *E. coli* bacterial clones as a model heterogeneous population. After one pass through the device, the concentration of one clone was increased from 0.32% to 98.6%, and a second clone from 0.11% to 95.6%. The combination of dielectrophoretic and magnetic modalities enabled multi-parameter selection akin to FACS sorting with multiple fluorescent channels and high throughput akin to MACS sorting. Yan et al.<sup>53</sup> designed a chip utilizing “DEP-active hydrophoresis”, to sort a mixture of viable and non-viable Chinese Hamster Ovary (CHO) cells in two distinct fractions, achieving 99.6% purity of viable CHO cells. The group leveraged hydrophoretic (size) and dielectric based separations simultaneously to achieve high purity. The last three works demonstrate that combining separation modalities can offer a significant advantage such as higher throughput, specificity, and/or purity, compared to standalone modalities.

The use of DEP to sort live and dead cells is a common application and serves as a label free alternative to flow cytometry. Xing and Yobas<sup>54</sup> utilized DEP to separate live and dead human colorectal carcinoma cells to achieve a 90% capture efficiency of live cells. In a recent work, Wei and coworkers<sup>55</sup> utilized DEP based separation to demonstrate high transfection efficiency of neurons via electroporation while maintaining cell viability. Highly efficient transfection via electroporation is achieved via high electric fields and thus typically results in cell damage. Wei coupled flow through electroporation with downstream DEP sorting on a chip to circumvent the need for a compromise between transfection efficiency and cell viability. There are many more examples of DEP based cell sorting in addition to those discussed above.<sup>56–59</sup>

**Electro-osmotic Flow**—Akin to the previously discussed EP and DEP sorting mechanisms, electro-osmotic based separation also results from an applied electric field. However, the process is phenomenologically different. Electro osmotic flow (EOF) refers to fluid movement by inducing solvated ion transport under an electric field. Suspended particles accompany the secondary fluid movement induced by migrating solvated ions (Figure 4C). Dittrich and Schwille<sup>60</sup> demonstrated a sorting microchip with pump driven primary flow and fluorescence triggered EOF sorting mechanism. This approach leveraged pressure driven flow to achieve a fast and stable flow, resulting in high throughput. EOF has also been used to augment a size based separation technique termed hydrodynamic spreading. Wu et al.<sup>61</sup> combined electro-osmotic flow with pump driven primary flow in order to augment hydrodynamic spreading and separate *E.coli* and yeast cells. Similarly, Kawamata and coworkers<sup>62</sup> demonstrated purely EOF driven separation of 1.0, 2.1, and 3.0  $\mu\text{m}$  particles. The advantage of EOF is typically the precise control of volumetric flow through various channels occupying the same microfluidic device. However, EOF requires fabrication of on chip electrodes, which adds complexity to chip manufacturing. Complications of secondary electrophoretic cell movement can accompany electro-osmotic driven pumping. Additionally, cell exposure to electric fields may result in reduced cell

viability. Nonetheless, this method enables precise control of small volumes of reagents and size based cell separation.

**Acoustic**—Acoustic based sorting has recently emerged as an additional modality that has no impact on cell viability.<sup>63</sup> At their core, acoustic separation modalities (*i.e.* acoustophoresis) work by inducing cell movement in response to an acoustically generated pressure wave. There can be several sub distinctions of acoustic cell sorting depending on the wave type; bulk standing waves, standing surface acoustic waves, and traveling waves.<sup>37</sup>

Bulk standing waves are generated within microfluidic channels when the applied wavelength matches the spatial channel dimension. As a result, two distinct regions are generated across the channel, along the wave's path. The first is termed a node, where there is no pressure fluctuation. The second is termed an antinode, where there is a fluctuating pressure alternating between a minimum and maximum (Figure 5A). Particles flowing through the channel will respond to the standing wave depending on their acoustic contrast factor, which is dependent on cell density and compressibility relative to the surrounding medium. Cells with a positive acoustic contrast factor will migrate toward the node and cells with negative acoustic contrast factors will migrate toward the antinodes, allowing for cell separation via different outlets.

Johansson et al. designed the first FACS device to sort cells<sup>64</sup> using standing waves generated by an automated fluorescence triggered transducer. The device offered a label free and gentle cell sorting technique. However, only a sort rate of 27 cells s<sup>-1</sup> was achieved, significantly lower than FACS. Jakobsson<sup>65</sup> also developed a microchip FACS to achieve binary particle sorting based on fluorescence detection. The chip also featured an acoustic 2-D pre-focusing zone that improved optical detection, sorting accuracy, and overall throughput to 150 particles s<sup>-1</sup>. Jakobsson's approach was only capable of binary sorting. To overcome this limitation, Grenvall et al.<sup>66</sup> fabricated a microchip with a 2-D, acoustic focusing zone to sort cells into five outlets based on their size. The device was used to fractionate leukocytes into high purity fractions with high total recoveries. However, a throughput of 150 cells s<sup>-1</sup> was not a significant improvement compared to other groups. Since mammalian generally exhibit a positive acoustic contract factor, they typically align at the nodes and most groups exploit this fact to sort cells. In an alternative approach, Shields et al.<sup>67</sup> synthesized elastomeric particles with negative acoustic contrast and showed that bio conjugation of mammalian cells to these particles could be used to selectively move cells to the antinodes within a microfluidic channel. As such, labeling one cell type among a heterogeneous cell population would allow sorting without a fluorescence trigger.

Standing surface acoustic waves (SSAW) are standing waves formed along the bottom of a microfluidic channel using inter-digital transducers (IDTs). The IDTs are patterned on a piezoelectric substrate, which is mounted to a microfluidic device. The wave changes modes from a transverse to a longitudinal wave from the substrate to the fluid, and these longitudinal waves create pressure nodes (Figure 5B). SSAWs are capable of deflecting an object in fluid flow independent of its contrast factor, and thus are thought be more flexible in separating cell populations that are small and inherently difficult to sort via bulk standing waves.<sup>68</sup> Li et al.<sup>69</sup> designed a SSAW based device capable of sorting water in oil droplets

into five different outlet channels. This type of device could be utilized as an upstream sorting component for droplet based genomic and transcriptomic analyses.

Most reports of acoustically driven cell sorting rely on standing waves, but traveling waves have been used to sort cells as well. Standing waves require wavelengths comparable to microfluidic channel width, and therefore the sorting rate cannot be increased because the wave frequency is constrained. Traveling waves offer a workaround to this limitation. Recently, Schmid and coworkers<sup>70</sup> designed a microfluidic device using fluorescence triggered traveling waves to sort cells into one of three channels (Figure 5C). Schmid reported a rate of 3000 cells s<sup>-1</sup> compared to 222 droplets<sup>69</sup> s<sup>-1</sup> via SSAWs. Similar to electrically driven cell sorting, acoustophoresis typically requires integrated transducers. This in turn complicates chip fabrication, operation, and increases cost. Furthermore, cell sorting via bulk standing waves is unsuitable for sorting subpopulations of the same cell type with similar contrast factors. In this case, a fluorescent label may be necessary to distinguish between subpopulations, thereby negating the label free advantage. However, acoustophoresis mitigates concerns regarding decreased cell viability which is frequently observed with electrical cell sorters and therefore the benefit of delicate cell handling may override cost and time concerns. Many more examples of acoustic based cell sorting are available and we refer the reader to focused reviews<sup>71-72</sup> for further discussion. In addition to acoustic and electrical forces, researchers have utilized alternative biophysical cues such as optical or radiation forces to sort cells.

**Optical**—The use of light to move particles dates back more than 45 years<sup>73</sup> when it was discovered that a focused laser could propel micro particles in a liquid. About 15 years later, the same researchers<sup>74</sup> achieved stable trapping via a tightly focused laser and this formed the foundation of contemporary “optical tweezers”. Optical forces result due to momentum exchange between incident photons of light and the irradiated object. Light scattering and absorption due to incidence with an object changes the light’s direction and magnitude and therefore the associated photons’ momentum. To achieve large displacements, many photons are called into action by using a focused laser. The particle’s behavior is dependent on its refractive index compared to the surrounding fluid, much like DEP is dependent on electrical permeability. When the particle’s refractive index is higher than the surrounding fluid, the particle will migrate toward the region of highest light intensity and vice versa. In both instances, the particle will move in the direction of light propagation as well. More detailed discussions on the physics of light induced forces can be found elsewhere.<sup>75-76</sup>

Since its inception, optical manipulation has been used to sort and manipulate cells on microfluidic chips (Figure 6A). Optical approaches to cell sorting are minimally detrimental to cell viability, in contrast to sorting via an electrical field.<sup>77</sup> Bragheri et al.<sup>78</sup> reported a device with a fluorescence triggered optical mechanism which deflected cells toward a specific outlet. However, the device could only sort approximately 100 cells per minute due to the lag in software communications as reported by the authors. Low throughput limits the application to smaller or less dense cell suspensions. Indeed, one of the major drawbacks of all microfluidic FACS systems is the slow throughput compared to conventional FACS that can sort at 10<sup>4</sup> cells per second. To address this issue, Chen et al.<sup>79</sup> reported a microfluidic device capable of sorting 23,000 cells per second with 90% purity and 45,000 cells per

second with 45% purity. The device utilized a tightly focused laser to induce a cavitation bubble in flow, which provided a mechanical force for cell deflection. The key innovation to achieving high sorting rates was a 3-D sheath focusing step made possible by a multilayered device structure. Two disadvantages to this approach was sample dilution due to the required sheath flow and the complexity of building 3-D microfluidic channels. The group improved on their initial design<sup>80</sup> by using an inertial based focusing step, therefore eliminating the need for 3-D device geometry. The devices discussed above utilized a laser focused at a fixed position in a microfluidic channel and therefore require focused single cell flows. In contrast, Wang and coworkers<sup>81</sup> eliminated the focusing step by integrating traditional optical tweezers in laminar flow. Eliminating the need for a focusing sheath flow simplifies device architecture and fabrication and also minimizes sample dilution, as previously discussed. Minimizing sample dilution is critical for assays with high detection limits.

**Magnetic**—Many of the discussed microfluidic systems have borrowed from conventional FACS systems in that a fluorescent signal acts as a trigger for an external force field to separate cells. Microfluidic magnetic based separations also borrow from their conventional MACS counterpart.<sup>32–33</sup> Cells are bio-conjugated to magnetic particles via a cell-specific antibody on the magnetic particle. These specific cells can be separated from a sample by passing the sample through a microfluidic device possessing a magnetic field or magnetized surface (Figure 6B). This method's simplicity and ability to separate via action at a distance is particularly advantageous compared to electrical cell sorters, which require electrodes in contact with the cell suspension. As previously discussed, this can lead to electrochemical reactions at the electrode fluid interface that may decrease cell viability or impact cell phenotype downstream.

The magnetic field can be induced via an external or integrated permanent magnet or an electromagnet. Capture via an external permanent magnet is common because of ease. For example, Wang et al.<sup>82</sup> isolated CTCs from whole blood by incubating whole blood with anti-EpCAM antibody functionalized magnetic nanoparticles. The incubated sample was introduced through a microfluidic device placed underneath a permanent magnet. Similarly, Besant and coworkers<sup>83</sup> isolated CTCs with magnetic nanoparticles and a permanent magnet but also integrated structures and channel design that captured CTCs with varying surface expression into designated zones. Chen et al.<sup>84</sup> combined both a bulk permanent magnet and patterned micro magnets in order to minimize the cell aggregation at the capture site. In contrast to the immobilization approaches discussed above, permanent magnets can deflect magnetic particles to an alternative outlet<sup>85–86</sup> for continuous flow sorting. Kim et al.<sup>87</sup> integrated a ferromagnetic wire array into the bottom of a microfluidic device so that an externally applied magnetic field was deformed resulting in lateral displacement of magnetically labeled cells. An alternative to using a permanent magnet is to use an electromagnet.<sup>88</sup> Electromagnets may offer an advantage in some separations because the magnetic field strength may be finely tuned by varying the current. However, device fabrication is more complicated and large currents can quickly generate Joule heating. The generated heat can increase sample temperatures above physiological temperatures and decrease cell viability. Furthermore, increased fluid temperatures can result in bubble

formation, which is problematic for functionality in microfluidic devices. To overcome this limitation, one can dissipate Joule heating by integrating dedicated cooling channel,<sup>89</sup> or using a highly thermal conductive substrate such as silicon to construct the chip.<sup>90</sup> Of course, both remedies add to the chip manufacturing cost.

Implementing microfluidic magnetophoresis typically requires antibody labeling. Immunolabeling can be problematic for several reasons: labeling may negatively impact post cells' endogenous genetic expression,<sup>35</sup> labeling may not be possible due to lack of surface markers, labeling may be undesirable because of clinical concerns, and antibodies are quite expensive. In some instances, the cell's native magnetic properties can be exploited for sorting as in the separation of red blood cells containing high levels of iron.<sup>91</sup> Some cells can be chemically treated in order to impart the desired magnetic properties. For example, Sofla et al.<sup>92</sup> devised a label free magnetic strategy to separate live cardiomyocytes by rendering the native myoglobin from diamagnetic to paramagnetic via oxidation with sodium nitrite. Microfluidic magnetophoresis based cell sorting has been applied extensively and the reader should refer to several recently published reviews.<sup>46, 93–94</sup>

**Passive Mechanisms**—The methods for microfluidic cell sorting discussed so far rely on an external force field to move cells. Methodologies that utilize intrinsic cell properties such as size, density, and deformability are discussed next. Passive mechanisms are particularly advantageous in that a fluorescent trigger to activate sorting is not required. Nor is external labeling as in magnetic based separations.

**Deterministic Lateral Displacement**—Deterministic lateral displacement (DLD) sorting uses a pillar array to direct cells one way or another based on cell size. Cells with a size less than a critical radius move in the direction of primary fluid flow. Cells greater than the critical radius are deflected in a direction determined by array design (Figure 7A). The critical particle size is dependent on the pillar design.<sup>95</sup> It has also been shown that cell shape and deformability can be exploited for DLD sorting.<sup>96</sup> This study extended the capability of DLD separation to discriminate between cells by morphology and deformability, in addition to size. However, only one post geometry was investigated, thereby neglecting the role of post geometry on cell separation. Ranjan et al.<sup>97</sup> explored the effect of the pillar shape in order to sort spherical particles, disc-shaped red blood cells, and rod-shaped bacteria. The study showed that rod shaped bacteria can be separated with 100% efficiency using “I-shaped” pillars and provided a method to separate non-spherical particles based on their longest dimension, adding to the microfluidic toolbox. DLD has also been used in other applications: to separate cancer cells from diluted whole blood,<sup>98</sup> erythrocytes of different phenotype as determined by deformability, leucocytes from erythrocytes, and subpopulations of leucocytes.<sup>99</sup> DLD is advantageous because it offers gentle, and label-free cell sorting and requires relatively facile fabrication to implement. However, the cells must differ in size or shape. For more on DLD, we refer the reader to a recent focused review.<sup>100</sup>

**Inertial**—Microfluidics, as the name implies, tends to occur in channels with micron sized channel dimensions. As a result, the dimensionless Reynolds number is typically small and inertial effects are often neglected. However, at modest channel dimensions or velocities, inertial effects manifest and can be exploited for cell sorting. One typical manifestation of

inertial effects in microfluidics is Dean flow,<sup>101</sup> which results in vortex formation perpendicular to the primary flow (Figure 7B). Cells with differing properties such as size, density, or shape respond differently to inertial effects and are focused at different channel locations. Cell sorting is achieved by splitting a single channel into multiple outlets. Recent reviews discuss the physics of inertial microfluidics in depth.<sup>101–103</sup> Warkiana et al.<sup>104</sup> exploited Dean flow in curved channels to sort label-free CTCs from blood with high throughput (1.7 mL/min), and conducted heterogeneity studies via DNA fluorescent in situ hybridization (FISH) post cell isolation. This method is advantageous because it is label free, and therefore can be used for various cancers lacking biomarkers. Furthermore, in contrast to magnetophoretic CTC separation that requires immunomagnetic labeling, this method may better preserve endogenous molecular expression and utilized a simpler workflow. In addition, a thorough mechanistic understanding of inertial microfluidics tends to be poorly developed leading to extensive trial and error during device development.

To address this limitation, Kim et al.<sup>105</sup> empirically investigated the effect of several parameters (channel height, width, radius of curvature, and flow rate) on inertial sorting in spiral microfluidics and then implemented these principles to design a two stage device to isolate CTCs from leukocytes. Using the results from the parametric experiments, the device was designed in one attempt, demonstrating and providing a toolbox for other researchers designing spiral inertial microfluidics. Recently, isolation of CTCs via inertial microfluidics has been demonstrated extensively.<sup>106–108</sup> Several sub categories of inertial microfluidic techniques are recognized such as field flow fractionation, pinched flow, and hydrodynamic spreading. A recent review discusses cell sorting via inertial microfluidics in depth.<sup>103</sup> Inertial microfluidics enable passive and label free cell sorting for instances when the target and non-target cells vary in size. Passive sorting simplifies device operation and fabrication, which is important for widespread adoption. Label free cell sorting is attractive for numerous reasons: minimized antibody related costs, applicability to cells lacking biomarkers, and maintaining integrity of endogenous expression. The last reason is critical for conducting high fidelity single cell molecular analyses. Furthermore, the methods are continuous, increasing throughput. A disadvantage is that most devices require diluted samples because cell-to-cell interactions manifest at high cell concentrations.

**Filtration**—In the chemical process industry, filtration is a well-established technique for size based separation. Several sub categories of filtration are in existence and are typically descriptive of the underlying process such as dead-end filtration, cross-flow filtration, microfiltration, ultrafiltration, etc. Likewise, scientists have long since implemented various filtration mechanisms in micro fabricated devices for cell enrichment. Weir filters (Figure 7C) offer a simple design; a single channel containing an obstruction that almost closes the channel permits only cells small enough to pass above the obstruction.<sup>109</sup> Pillar filters (Figure 7C) feature regularly spaced pillars in a micro channel which obstruct the passage of larger cells.<sup>109</sup> However, both filter types are only useful for low density samples or small sample sizes because they are prone to clogging, akin to dead-end filters in the chemical process industry. To address this limitation, scientists have micro fabricated cross-flow filters, which have filter elements parallel rather than perpendicular to the main flow direction. The main fluid flow sweeps across the filter in order to clear clogged cells. Cross

flow filters (Figure 7C) have been used for the separation of myocytes and non-myocytes,<sup>110</sup> leukocytes,<sup>111</sup> bacteria,<sup>112</sup> and CTCs from blood.<sup>113</sup> In another approach to eliminate clogging, McFaul et al.<sup>114</sup> incorporated a periodic backflow to reduce clogging in a micro fabricated cross flow filter. Filtration based microfluidic cell sorters are relatively easy to fabricate, operate continuously, and label free. However, they are only capable of sorting cells differing in size.

**Outlook for Microfluidic Cell Sorting**—Microfluidic cell sorting is a mature research field, and was well established even prior to the paradigm shift toward single cell analysis. For brevity, we have only discussed the most prevalent modalities for microfluidic cell enrichment. Other approaches implemented include use of valves,<sup>115–116</sup> transient cell adhesion,<sup>117</sup> and permanent cell immobilization.<sup>118–119</sup> Despite the field's maturity, researchers continue to innovate and conceive new techniques for cell separation. In fact, researchers are enriching cells in creative ways that are not easily categorized. Wang et al.<sup>120</sup> demonstrated a microfluidic device for cell enrichment on the basis of cell viscosity. The device demonstrated fractionation of two leukemia cell lines as well as leukemia cells from healthy leukocytes. Zhang et al.<sup>121</sup> exploited the difference between surface free energy between two microbial cells to accomplish enrichment. As evidenced, we expect the field of microfluidic cell enrichment to continue growing.

Among the many discussed works, most were examples of standalone microfluidic cell enrichment. FACS remains a powerhouse for microfluidic enrichment prior to single cell analysis. This may be for several reasons; high throughput ( $10^4$  cells per second), facile integration with single cell compartmentalization (well plates), time tested (invented in 1969), high purity (95–100%), multiple and simultaneous sorting criteria, etc. FACS itself is a means of single cell analysis in conjunction with hybridization techniques. In contrast, FACS has shortcomings that can be addressed via a micro fabricated system such as large sample size requirements, low total recovery, large footprint, and high costs. So what factors prevent wider adoption of microfluidics? Limited throughput is a key factor. Modalities, which are amenable to continuous flow and trigger free enrichment, promise the highest throughput. If a single chip cannot offer competitive throughput, scaling strategies such as chip parallelization need to be implemented. Additionally, microfluidics is not readily reusable due to clogging and cell adhesion. Perhaps, microfluidic platforms will find a niche in the sterile single use market. To do so, investment in manufacturing and validation is required. We anticipate wider adoption as these issues are addressed and systems are commercialized.

### C. Single Cell Isolation

**Conventional Approaches**—After obtaining an enriched cell suspension, the next step in the workflow is to isolate single cells from one another for analysis as discrete individuals. Single cell immobilization is inadequate on its own. Cells must be compartmentalized in such a way so lysate contents of one cell do not contaminate another, allowing true single cell analysis. As already discussed, FACS can be used as a method of both sorting cells and addressing single cells into an individual micro well for molecular analysis.<sup>31, 122</sup> FACS based cell compartmentalization is high-throughput, automated and

micro wells can be easily accessed for reactant addition or product collection. The disadvantages, as previously discussed, are high cost and large sample volume requirements. Furthermore, wells open to the environment introduce a contamination risk. Nevertheless, FACS remains a staple, commercial technology.

Micromanipulation is a technique that involves manually selecting and transporting a single cell of interest to its own container for downstream workup. One way to do so is mechanically, via a pipette (Figure 8A). A particular advantage of micromanipulation is that cell enrichment is not required since cells may be visually identified prior to manual selection. Manual identification and selection under a microscope ensures a high confidence level that a single cell has been compartmentalized. Selection via micromanipulation can also be done in combination with FISH to discriminate cells by specific genetic features.<sup>123</sup> Additionally, micromanipulation is well suited for small sample sizes of fragile materials. However, micromanipulation is low throughput and is also done in an open environment, thereby risking contamination. Citri et al.<sup>124</sup> demonstrated picking up single neuron cells for quantitative PCR (qPCR) analysis. Recently, Marinov et al.<sup>5</sup> quantified stochastic RNA expression in a lymphoblast cell line using micromanipulation for cell isolation and an RNA-sequencing technique. Pipette micromanipulation is commonly utilized due to its simplicity and low price and commercially available automated systems can increase throughput.<sup>125</sup>

Optical tweezers, as discussed above in regards to cell enrichment (Figure 6A), are also categorized as a micromanipulation technique and are readily used for compartmentalizing a single cell. This mechanism harnesses the momentum of refracted and scattered light photons to position a particle at the center of the light's focus.<sup>75-76</sup> Optical tweezing for single cell isolation prior to molecular analysis has also been demonstrated.<sup>126-127</sup> The main advantage of utilizing optical tweezers compared to mechanical micromanipulation is volume reduction - equal to approximately the cell volume itself. This minimizes lysate dilution and therefore increases assay sensitivity. A second advantage is contactless cell compartmentalization, thereby minimizing contamination risk. However, optical tweezers suffers from low throughput akin to mechanical micromanipulation.

A crude but simple method for single cell compartmentalization is serial dilution (Figure 8B). This involves step-wise dilution of a cell suspension until single cells are obtained in individual vessels.<sup>128</sup> Though cheap and simple, serial dilution can be laborious and unreliable, resulting in some fractions containing no cells, single cells, or several cells. Furthermore, batch wise processing introduces contamination risks.

Up to this point, all of the discussed techniques have been applicable for suspended cells. As a result, it is impossible to recognize the isolated cell's spatial origin in the starting intact tissue. This information is instrumental if attempting to correlate genetic or other molecular expression to cellular spatial distribution within native tissue. The ability to spatially map single cell data would greatly increase our understanding of complex heterogeneous tissues, far beyond solely cell type enumeration. Coupled with a temporal analysis, researchers could study how molecular processes propagate throughout various tissues. Practical applications include studying embryonic development, and comparing healthy and diseased



tissue to identify new therapeutic targets. Laser capture micro dissection (LCM) is a powerful technique, developed for isolating single cells from their heterogeneous, native tissue environment while preserving their spatial origin.

In the LCM technique, a thermoplastic film is attached to a tissue section and the tissue section is placed tissue-side down on a glass slide. The glass slide is positioned on an inverted microscope for imaging and a plastic cap is placed over the plastic film. Once cells of interest are identified via microscopy, a focused infrared laser melts the plastic film over the cells, thereby adhering the cells to the film (Figure 8C). When the cap attached to the film is removed, the cells of interest are sheared from the intact tissue and transferred to the cap.<sup>129</sup> There are several commercial systems available with different laser types; infrared (IR), ultraviolet (UV), and combined IR/UV. The ultraviolet systems operate on a slightly different principle; a cell of interest is removed via UV laser by cutting around the cell rather than adhering to plastic.<sup>130</sup> As mentioned, LCM permits single cell isolation with knowledge of in situ origin. The technique allows direct visualization and morphological cell identification. Tissue are typically flash frozen and then cryosectioned, thereby providing a stable snapshot of gene expression for downstream molecular analysis. LCM is particularly advantageous when the number of cells to be isolated is too low to use FACS. As such, LCM has been used extensively for single cell molecular analysis.<sup>131–133</sup> With continued method development, systems such as the Bio-Rad Clonist<sup>TM</sup> can now isolate live cells, rather than exclusively frozen or fixed samples. Despite its wide adoption, LCM is not without disadvantages. The technique is low throughput compared to FACS and an instrument can cost around \$150,000. The protocol is performed at least partially in an open environment, thus again, risking contamination. Morrison et al.<sup>134</sup> compared LCM and FACS in regards to isolating and measuring single cell gene expression in the avian embryo and showed FACS to be advantageous. The study showed that 96% of FACS isolated single cell generated usable gene expression profiles compared to ~60% of LCM isolated cells. Furthermore, with an optimized FACS protocol, native gene expression can be preserved and is highly correlated with that from LCM isolated cells. Despite some drawbacks, LCM remains the only technique capable of in situ single cell isolation.

Many challenges of single cell analysis are encountered in compartmentalizing single cells. Ideal methods would be both high-throughput and low cost, two requirements that usually oppose each other. At the same time, single cell compartmentalization must remain efficient for smaller samples. Dilution must be minimized in order to enable assays such as the analysis of low protein or transcript quantities. Furthermore, contamination effects become amplified at low analytic quantities and must be avoided. Extreme care should be taken at this juncture to assure a high fidelity and non-biased result. In the next section, we discuss how microfluidic devices are employed for single cell compartmentalization.

**Microscale Approaches**—Microfluidic devices offer many advantages to achieving single cell compartmentalization. Single cell compartments are miniaturized to reduce lysate dilution. This is critical for assaying low abundance biomolecules such as mRNA which can be present at 0.01–2.5 picograms per single cell.<sup>135</sup> Reagent volumes are minimized, thereby decreasing cost. A high surface area to volume ratio ensures high heat transfer and temperature control, critical for PCR assays requiring temperature cycling.

Compartmentalized cells can be closely arrayed allowing for facile visualization via microscopy. Furthermore, many microfluidic solutions are completely hands-free, closed systems, minimizing contamination risk. For example, *Fluidigm's* C1 Array is a state of the art, commercial microfluidic product for automated single cell isolation. Cells are introduced into the chip, in which they follow a serpentine pattern through each available capture site. Once a cell occupies a capture site, subsequent cells bypass the occupied site and are trapped at the next capture site. Trapping can be followed by reagent addition for single cell reverse transcription and amplification. Marcy et al.<sup>136</sup> reported microfluidic DNA amplification to be highly advantageous due to reduced amplification bias, higher analyte specificity, and better economies of scales in nL volumes. In the following sections, we review microfluidic compartmentalization for single cell analysis. The focus is predominantly on designs for molecular single cell analysis. We briefly review trapping methods that do not isolate single cell lysates but can be used for microscopic analysis of single cell dynamics. For a discussion on additional cell trapping mechanisms, we refer the reader to a previously written review.<sup>137</sup>

**Valves**—On chip valves offer an easily conceptualized system for single cell trapping. Additionally, valves can be used to both regulate fluid flow and control flow direction. Quake et al. popularized the commonly used microfluidic valve architecture, frequently termed the Quake valve.<sup>138–139</sup> Using Quake valve architecture, Streets et al.<sup>140</sup> investigated gene expression in mouse embryonic cells and mouse embryonic fibroblasts using RNA-sequencing on a microfluidic chip. Single cells were trapped between two pressure actuated valves in a chamber of only 0.86 nL. Subsequent steps were also performed in similar chambers of 1.35–128 nL. The authors attributed the high experimental reproducibility to the use of microfluidics, which reduces stochastic variation due to pipetting errors and handling. Reagent mixing was accelerated by actuating the valves independently in a back and forth fashion. Shi et al.<sup>141</sup> designed a chip containing 120, 2.0 nL micro-chambers isolated by push-down valves. The chambers were used to trap single cells and analyze each cell's protein content via a patterned antibody array within the chamber. Fan et al.<sup>142</sup> utilized a microfluidic chip to isolate a single cell, lyse the cell, and partition the resulting chromosome suspension into 48 different cell chambers for amplification, allowing for genome wide haplotype analysis. The cell and chromosomes were compartmentalized in discrete chambers by pressure actuated valves on each chamber. Similarly, White and co-workers<sup>8</sup> designed a chip single cell digital PCR analysis. The device was used to analyze 200 single cells on a 10 cm<sup>2</sup> chip and was operated by controlling twelve pneumatic valves independently. Recently, Sun et al.<sup>143</sup> designed a chip for single cell reverse transcription quantitative PCR (RT-qPCR) to investigate the effects of methyl methanesulfonate on human cancer cell (MCF-7) gene expression. The chip trapped a single cell between two pneumatically controlled valves. The microfluidic method increased assay sensitivity and gene upregulation was detected after 27 amplification cycles.

While on chip valve systems are easily conceptualized, all of the above examples were two layer pneumatic valves, or Quake valves. The bottom microfluidic layer houses channels for cells, buffers, and reagents and the top microfluidic layer houses larger channels that perpendicularly intersect the underlying channels. The larger channels are pneumatically

pressurized and force the bottom channels to close (Figure 9A). In addition to two-layer architecture, these devices typically employ computer controlled pneumatics. Both characteristics complicate device fabrication, operation, and increase cost. Finally, single cells may be loaded via pipette injection or syringe pumped flow but require a user to confirm single cell trapping via microscopy, limiting throughput. Micro valve performance has advanced significantly in regards to cost, leakage, minimizing volume, and fabrication options. Work towards automatic feedback controlled valves coupled with microscopy would enable completely hands off single cell analysis and increase throughput significantly.

**Dielectrophoretic**—Dielectrophoretic methods to compartmentalize single cells have been applied with great success. In fact, DEPArray™ System (Figure 9B) from *Silicon Biosystems* is a commercial microfluidic system for single cell isolation. The system includes a single use cartridge and analysis platform. The cartridge is an array of individually controllable electrodes enabling single cell trapping via DEP cages. Post trapping, cells are visually identified and manipulated to other traps or isolated off chip. The system has been recently used for isolating single lung and breast cancer cells from patient blood samples<sup>144–146</sup> in order to perform sequencing and RT-qPCR. Using the DEPArray™, Carpenter et al.<sup>147</sup> isolated single patient derived neuroblastoma cells for genome sequencing. In this approach, the researchers moved single cells into a microtube or other container post on chip DEP trapping and identification. Thus, strictly speaking cells are not compartmentalized on chip. For the same reason, the method is relatively low throughput, limiting applications to smaller samples and increasing labor costs. Furthermore, multiple single cell measurements are necessary to distinguish true cell heterogeneity from experimental noise.

**Microwells**—Microwells provide a facile way to isolate single cells using physical boundaries, akin to how multiwell plates physically isolate cell groups (Figure 9C). The key difference between microwells and conventional multiwell plates is smaller well size and volume. Microwells for single cell isolation have been previously reviewed in detail.<sup>148–149</sup> Cells are typically seeded into individual microwells by gravitation and cells remaining outside of the wells are flushed away. One drawback is that typically single cells will occupy only a fraction of the wells; the rest may contain more than one cell or no cells. However, adjusting well size, shape, and cell concentration can optimize the single cell seeding efficiency. Large arrays can be fabricated to ensure enough single cells are trapped for meaningful analysis. Some experiments demonstrated simultaneous use of DEP and micro wells to control cell seeding.<sup>150–151</sup> Despite facile fabrication and operation, micro well approaches are more suitable for microscopic single cell studies rather than molecular analysis, since cell lysates may mix.

**Hydrodynamic**—Single cell trapping can be accomplished by passive, hydrodynamic mechanisms. This approach is attractive because it does not require sophisticated experimental systems such as DEP or valve based systems. There are several sub categories to hydrodynamic trapping. The terms “eddies” and “vortices” are interchangeably used to describe trapping induced by recirculating fluid flow. In one example, it was demonstrated

that four recirculating eddies induced by an audible frequency fluid oscillation around a cylinder can be used to trap single cells at the eddy centers.<sup>152</sup> The effect was termed “hydrodynamic tweezers” (Figure 9D). The same laboratory investigated non cylindrical geometries and showed that device geometry and oscillation frequency controls the eddy number, shape, and strength.<sup>153</sup> Tanyeri and Schroeder<sup>154</sup> demonstrated controllable, 2-D, hydrodynamic particle steering by adjusting flow rates at a junction of four buffer streams. Additionally, a permanently stable stagnation point was demonstrated wherein the trapped particle is not displaced by Brownian motion. Cell lysates are not isolated via this method; therefore the utility of hydrodynamic tweezers is geared toward microscopic analysis. However, Hayakawa et al.<sup>155</sup> used vibration induced flow around spirally arranged micro pillars to capture a single cell in a patterned thermo-responsive gel. After a single cell is captured at the gel center, the chip is cooled and the expanding gel closes over a single cell, resulting in compartmentalization. But, the method reported only a 60% cell capture success rate with 61% of captured cells remaining viable. For further discussion of vorticity based cell trapping, we refer the reader to a recent review.<sup>156</sup>

A second passive hydrodynamic trapping method uses physical obstructions such as U-shaped cups to physically isolate single cells on chip (Figure 9E). The obstructions may have cutaways allowing fluid flow through an unoccupied trap, thereby increasing trapping occurrence. An early example was demonstrated by Di Carlo<sup>157</sup> who used an array of physical U-shaped traps to isolate 100 single human cervical carcinoma cells and performed on-chip for 24 hours. This approach has been modified and implemented for various applications such as; trapping and culturing single *E. coli* cells,<sup>158</sup> human dermal fibroblasts,<sup>159</sup> trapping and selective exposure of single hepatocytes via co-flowing streams,<sup>160</sup> and lymphoma cell capture for microscopic analysis of cellular markers via antibody staining.<sup>161</sup> Recently, Guan et al.<sup>162</sup> published a comprehensive design procedure for designing devices for single cell hydrodynamic trapping. They demonstrated the design of a device with 100% capture efficiency and confirmed their finite element simulation results with experiments. All of the experiments discussed above utilized a flow perpendicular to the trap. Another derivative of this technique utilizes flow tangential to traps.<sup>163–164</sup> Espulgar et al.<sup>165</sup> designed a device for trapping single cardiomyocytes to observe cell growth, coupling and beating. Uniquely, the cell loading method did not require a pump to drive cells into traps; instead cells were pipetted into the device and the device was centrifuged to trap cells. Another format for hydrodynamic single cell trapping was recently demonstrated by Jin and coworkers.<sup>166</sup> The authors demonstrated 100% cell trapping with HeLa cells. The device design provides deterministic single cell trapping akin to that demonstrated by Guan et al.<sup>162</sup> However, this format does not require long bypass channels to achieve optimum flow resistances. The isolation methods utilizing hydrodynamics and physical obstructions as discussed above are beneficial because they are passive and can be adopted for various cell sizes and shapes. However, almost all works used trapped cells for culturing and transient imaging analysis, rather than single cell lysate analysis. Nevertheless, these methods can be coupled with FISH for single cell genomics.<sup>167</sup>

**Droplets**—Droplets have emerged as a popular means for single cell compartmentalization (Figure 9F). Monodisperse droplets are generated by co-flow of two immiscible fluids.<sup>168</sup>

This methodology is especially useful for molecular analysis of single cell lysates, as each drop can function as an independent chemical reactor.<sup>169–170</sup> Using droplets eliminates complex fabrication requirements such as two layer valve systems, or integrated electrodes for DEP systems. Droplet generation and cell encapsulation is done in continuous flow, enabling high throughputs, typically up to several kHz.<sup>169, 171</sup> Picoliter<sup>169–170, 172</sup> or femtoliter<sup>173</sup> droplets are achievable, thereby reducing dilution of analytes present in low quantity. Zinchenko et al.<sup>169</sup> continuously compartmentalized single E coli cells in droplets for a directed evolution experiment to create clones with higher enzyme activity. The cells were encapsulated together with substrate and lysing chemicals to produce a fluorescent reaction indicative of each cell's enzymatic activity. Each droplet was then detected and sorted via FACS to isolate the best clones. Recently, Lim and coworkers<sup>172</sup> compartmentalized single E coli cells on chip and conducted in-droplet single cell PCR. The droplets were then sorted based on fluorescence intensity correlating to the PCR assay. The authors termed the technique “PCR active cell sorting” or PACS. As shown in the preceding two examples, droplet based cell compartmentalization can also be integrated with detection and sorting strategies.

Droplet based approaches compartmentalize cells according to a Poisson distribution, meaning that more than half of droplets will be empty.<sup>172</sup> Some studies have reported approaches to beat Poisson statistics and increase single cell compartmentalization efficiency. For example, Ramji et al.<sup>174</sup> developed a device with an initial stage in which lung cancer cells are disaggregated, focused, and uniformly spaced through a series of expanding and contracting channels. Then, single cells are combined with reagents and encapsulated in droplets. Their experiment resulted in a single cell encapsulation efficiency of 55% and only 25% of droplets were empty. The platform was utilized to study single cell activity of the epidermal growth factor receptor, an indicator of cancer metastasis. Kemna et al.<sup>175</sup> utilized Dean flow in a spiral micro channel for cell pre-focusing and reported a single cell encapsulation efficiency of 77%. The preceding two examples optimized cell focusing and spacing prior to the compartmentalization junction in order to increase efficiency. Jing et al.<sup>176</sup> noted that these approaches require cell high cell densities ( $10^7$  cells/mL), potentially limiting their clinical application. The group designed a two stage device consisting of droplet generation and DLD droplet sorting. The droplet generator produced empty 14  $\mu\text{m}$  diameter droplets, which increased to 25  $\mu\text{m}$  after single cell encapsulation. The DLD stage then sorted empty droplets from those containing single cells. The device generated droplets at 5 kHz with 80% single cell encapsulation efficiency. Additionally, only a 100  $\mu\text{L}$  low density ( $10^4$ – $10^7$  cells/mL) sample is required. The device was used for assaying single lung cancer cell matrix metalloproteinase secretion. Metalloproteinase secretion was investigated using a predetermined calibration curve, spanning enzyme concentrations from 5 to 64 nM.

As evidenced above, increasing single cell compartmentalization in droplets can be achieved via pre focusing or post sorting steps. In fact, facile integration of droplet formation with other steps enables applications other than molecular assays. Schoeman and co-workers<sup>177</sup> demonstrated single cell droplet encapsulation followed by fusion of two droplets to produce a hybridoma, a fusion of myeloma and B-cells. The device featured two inlets for introducing the two different cells. Each cell traversed an “alternating spiral microchannel”

for cell pre focusing. Then, each cell was encapsulated in a droplet at a T-junction, operating such that the cells are encapsulated by alternating cell type. The two paired droplets then pass on chip electrodes which induce droplet coalescence. Next, the coalesced drop is reduced in size through contact with a “pitch-fork” structure to promote cell-to-cell contact. Finally, the two cells are electro fused via on chip electrodes. This study demonstrated the versatility of droplet microfluidics, beyond cell assay applications.

Droplets have emerged as a powerful platform for single cell biology. Single cell molecular assays such as PCR and fluorescence based protein assays have been miniaturized and compartmentalized into picoliter droplets. The yearly publication number regarding single cells and droplet microfluidics has more than doubled over the last 5 years. As such, we can expect considerable growth in this research field. For more applications and information regarding single cell droplet microfluidics, we refer the reader to several focused reviews.<sup>178–179</sup>

#### D. Single Cell Lysis

**Conventional Approaches**—Once a single cell of interest is compartmentalized, and the biomolecule under investigation is identified, the next step is quantifying the target. Transmembrane proteins are frequently quantified via fluorescent antibody probes. In contrast, biomolecules within the cell are typically extracted for assay. To extract the molecule, the cell plasma membrane must be disrupted. The nature of the plasma membrane varies across cell types and organisms. Conventional methodologies for membrane disruption can be classified as detergent and non-detergent based. Non-detergent based approaches include mechanical agitation, liquid homogenization, temperature cycling, and sonication. Traditional mechanical cell lysis relies on rotating impeller blades, a mortar and pestle,<sup>180</sup> bead beating,<sup>181</sup> or a homogenizer<sup>181</sup> to break open cells. However, these methods are not suitable for single cell lysis, but rather are appropriate for many cells in suspension or larger tissue samples. Gunerken et al.<sup>182</sup> recently reviewed these and other lysis techniques as they apply to lysing microalgae for biorefineries. Sonication disrupts the cell membrane via high frequency sound waves generated by an immersed piezoelectric transducer. Cheow et al.<sup>183</sup> lysed single liver cancer cells confined in nanoliter wells by immersing the well plate in an ultrasonic bath. However, sonication typically requires 50 seconds for single cell lysis and in that time, can generate enough heat to denature proteins.<sup>184</sup> Pretreatment with a non-ionic detergent shortened the required time to only 3 seconds.<sup>184</sup> Additionally, heating can be prevented by utilizing short discontinuous bursts instead of continuous sonication and by sonicating in an ice water bath. A freeze-thaw cycle can also be used to lyse cells. Ice crystals formed during freezing contract during thawing to break cells. Kim et al.<sup>185</sup> evaluated freeze-thaw lysis of single lymphocytes for DNA extraction where the cell was frozen in 10  $\mu\text{L}$  of purified water via liquid nitrogen and thawed at room temperature. The cycle was repeated twice. Multiple cycles are typically necessary and as such, the freeze-thaw approach can be lengthy.

Detergent based cell lysis is a potentially milder and quicker approach compared to mechanical, sonication, and freeze-thaw cell lysis and can be scaled down for single cells. Detergents lyse a cell by solubilizing proteins associated with the cell plasma membrane and

disrupting interactions between lipids and proteins. A variety of detergents are available, characterized by the nature of their hydrophobic tail and hydrophilic head. Detergent selection is empirical. However, general rules are useful; nonionic or zwitterionic detergents are less denaturing compared to ionic detergents and are therefore used when maintaining native protein structure or function is important. Though, a milder detergent will require longer exposure times for cell lysis and could confound transient biomolecule expression in single cell studies. For example, Han et al.<sup>186</sup> tested various detergents and concentrations for their ability to lyse a single cell while maintaining the nucleus intact. A non-ionic detergent, Triton, at 2% was able to lyse the cell membrane within 10 minutes of exposure and maintain an intact nucleus for up to one hour. Shoemaker et al.<sup>187</sup> lysed single cells with 0.1% of Triton X-100 for subsequent enzyme activity analysis. As evidenced above, detergent based lysis protocols require precise liquid handling for accurate data interpretation, and careful selection of optimal lysis media.

A frequent goal of cell lysis is to minimize alteration of a molecule's native structure and expression. This means that the approach must be both gentle and rapid, normally confounding requirements. Sonication, freeze-thaw, and detergent based methods are applicable for single cells, though each may have their disadvantages: excessive heat generation, long protocols, and arduous implementation. Microfluidic technology has enabled new cell lysis approaches, specifically suited for single cells.

**Microscale Approaches**—Microfluidic devices provide an ideal platform for single cell lysis. Devices can be manufactured with unique geometries and precise dimensions and operated in the laminar flow regime. This allows for finely tuned mechanical or chemical single cell perturbation. Microfluidic dimensions on the length scale of single cells minimize lysate dilution increasing assay sensitivity. Laminar flow characteristics minimize convective transport of lysate. Most devices are optically transparent, allowing for visualization. Devices are typically contained, minimizing contamination for sensitive molecular assays such as PCR. There are several microfluidic single cell lysis methods and each has its own merits. Selecting the appropriate technique is dependent on many factors akin to conventional cell lysis, and is crucial for achieving the desired result. In the next sections, we discuss select single cell lysis modalities highlighting recent experiments. For further discussion of microfluidic cell lysis, we refer the reader to two focused reviews.<sup>188–189</sup>

**Mechanical**—Mechanical cell lysis punctures cell membranes via a mechanical force. The force can be induced by shear, compression, collision with sharp features and other methods. Kim et al.<sup>190</sup> devised a fabrication method enabling spatio-specific and reversible channel formation on a microfluidic chip, following mechanical strain application and release. The group demonstrated single cell lysis using the new technology. Briefly, channels were created via applied strain and a single cell was placed in the newly formed channel. Following strain release and channel collapse, the single cell was lysed via compression. However, this early phase demonstration required manual handling and placement of single cells into the channels. Hoefemann et al.<sup>191</sup> demonstrated single cell lysis in continuous microfluidic flow. Cells passing over an integrated heater were lysed by heat generated

bubbles which compressed the cell against the channel ceiling (Figure 10A). Single cell lysis in less than 20 milliseconds was achieved with 100% efficiency. However, the experiment did not include a single cell assay, and therefore lysate diffusion or compartmentalization should be considered for single cell molecular analysis via this approach. The review by Nan and co-workers<sup>188</sup> discusses mechanical lysis further, though specificity to single cells is rare.

**Thermal**—Thermal cell lysis relies on heat induced denaturation of cell membrane proteins, thereby opening the cell. Thermal, single cell lysis for single cell PCR has been executed off chip using a standard thermocycler and PCR tubes<sup>192</sup>. The lysis step required a 95° C hold for 90 seconds. Thermal lysis can be preferable compared to chemical lysis when enzymatic or detergent contamination of the intracellular biomolecules is to be avoided. However, careful consideration and precise control of the temperature is required for heat sensitive molecules. As such, thermal cell lysis is rarely used for protein analysis. Instead, it is most frequently used for parallel, on-chip, PCR analysis that requires additional temperature cycling. For example, Gong et al. loaded 6086 single cells into on-chip wells and performed cell lysis by heating the chip to 50°C for 40 minutes.<sup>193</sup> Following thermal lysis, the temperature was cycled to amplify transcribed cDNA products. Another critical limitation of thermal lysis for single cell molecular analysis is the time required to achieve lysis. Given that thermal lysis typically occurs on a time scale of minutes, the technique is unsuitable for measuring intracellular signaling events, typically occurring within seconds.<sup>194</sup> This is another reason why thermal lysis is most frequently used to measure events such as gene expression, which occur over several hours.<sup>194</sup> Additionally, many droplet microfluidic platforms developed for continuous single cell PCR utilize heat lysis.<sup>172, 195</sup>

**Chemical**—Given its long history of application to bulk cellular analysis and facile scalability, chemical lysis is a popular technique for single cell lysis. Treutlein et al.<sup>33</sup> captured single cells for RNA sequencing and qPCR using the commercially available *Fluidigm* C1 system, which uses a lysis buffer to open cells. *Fluidigm* provides a proprietary lysis buffer or refers their customers to other commercial detergents such as Thermo Scientific's nonionic NP-40 detergent. Similarly, Streets et al.<sup>140</sup> fabricated their own microfluidic chip for single cell RNA sequencing. After trapping a single cell in a reaction chamber, the cell was lysed by addition of buffer containing 10% NP-40. Selecting the appropriate lysing protocol can be done by consulting manufacturers' guides for bulk cell applications, typically made available by companies providing lysing buffers. Furthermore, a plethora of scientific literature can guide appropriate reagent selection for mammalian,<sup>196</sup> bacterial,<sup>197</sup> and tissue<sup>198</sup> lysis.

Lysing speed can be dependent on many factors such as the detergent or enzyme being utilized, the concentration, and the contact efficiency. The former two parameters are partly constrained by the biomolecule of interest. Ionic detergents such as sodium dodecyl sulfate can lyse cells rapidly compared to non-ionic detergents such as Triton X-100, but will also denature proteins. In contrast, it is always desirable to maximize contact efficiency for faster cell lysis. Doing so can be particularly challenging in microfluidic systems. Micro scale



flows typically occur in the viscous flow regime, and as such, molecular transport and mixing is dominated by diffusion. Shi et al.<sup>141</sup> utilized Cell Lysis Buffer from Cell Signaling to lyse single cells isolated in microfluidic chambers. The lysis buffer was brought into contact with cells strictly via diffusion. The authors allowed 20 minutes for lysis buffer diffusion, and another 20 minutes for incubation. As already discussed, the length of the lysis process can limit the study of faster occurring intracellular events. To overcome this limitation, peristaltic pumps, syringe pumps, actuating valves (Figure 10B), or manual pipette injections are used to sequentially move reagents across cells and facilitate mixing.<sup>8, 33, 140, 142–143</sup>

The protocols discussed so far applied chemical lysis in discrete on chip chambers, formed by flanking pneumatic valves. This approach limits single cell analyses to “batch” wise operation. However, chemical lysis can be utilized for continuous single cell analyses by compartmentalizing the lysing buffer along with a single cell into picoliter droplets as already discussed. Hence, cell compartmentalization and lysis are performed simultaneously. For example, DeKosky et al.<sup>199</sup> encapsulated single lymphocytes along with lithium dodecyl sulfate in ~73  $\mu\text{m}$  diameter oil droplets by using a flow focusing nozzle and reported 100% lysis efficiency. Many more studies have reported the use of droplets for single cell compartmentalization and chemical lysis with application to RNA-sequencing,<sup>161, 200</sup> PCR,<sup>201</sup> and single cell enzyme activity.<sup>169</sup>

All of the single cell lysing methods discussed so far required cells to be in suspension so that they could be manipulated across the microfluidic platform. Thus, cells are removed from their native environments such as intact tissue or adherent cultures. This makes it impossible to correlate single cell data with their native context. We have already discussed the time scales of intracellular events,<sup>194</sup> therefore it can be expected that upon removing a cell of interest from its native context, cell surface receptor activation or protein modification would change before one could measure it. To address this limitation, Sarkar et al.<sup>202</sup> developed a microfluidic device to selectively lyse a single cell in adherent cell culture and capture its lysate while minimizing dilution. The device produces an outflow of lysis buffer at a device tip and the lysis buffer is hydrodynamically confined to an area on the scale of a single cell by a balanced surrounding inflow of lysis buffer (Figure 10C). The confining inflow also captures the cell lysate and delivers it to the assay chambers. To initiate an experiment, the device is positioned over a target cell in a standard tissue culture plate using a micromanipulator and the lysis buffer flows are controlled via two independent syringe pumps. While this approach is low in throughput, requiring manual and precise device positioning, it is unique in its ability to analyze single cell protein activity in adherent cell culture.

**Electrical**—The cell plasma membrane is composed of a lipid bilayer that serves to protect the cell from its exterior environment. Upon exposure to an electric field, the lipid bilayer undergoes molecular reorientation and thermal phase transitions and new pores are formed.<sup>203</sup> If the electric field is mild (0.2–1 V) and the exposure time is short, pore formation is reversible.<sup>203</sup> This is termed electroporation and is frequently used for loading therapeutic and genetic materials into cells.<sup>204</sup> In stronger electric fields or prolonged exposure, the pore formation is permanent. As the osmotic pressure between the cytosol and

the surrounding media becomes unbalanced, cells swell and rupture. The electric field can also be high enough to cause rapid cell rupture.<sup>205</sup> Electrical cell lysis offers a distinct advantage in that the electric field can be tuned for rapid cell lysis without denaturing target biomolecules. In fact, The difference between trans cell-membrane potential and trans organelle-membrane potential can be exploited to selectively rupture the cell membrane while leaving organelles intact.<sup>206</sup>

Mellors et al.<sup>207</sup> built a chip for single cell analysis of erythrocyte proteins via capillary electrophoresis and electrospray ionization mass spectroscopy. All flows on the chip were driven via electroosmotic pumping. An injected cell suspension traveled to a T intersection where an increase in the electric potential (4 kV) lyses cells. The authors found single cell lysing events occurring at a rate of 0.2 cells s<sup>-1</sup>. Young and co-workers<sup>208</sup> demonstrated a microfluidic device for EOF positioning and electrical lysis of a single lymphoma cell. Their method reported a success rate of 80% while taking approximately 60 seconds on average from cell injection to cell lysis. The method described by Young processed a single cell at a time. Bahi et al.<sup>209</sup> fabricated a chip capable to trap an array of single cells via pDEP at 1 V potential, followed by lysis via a 60 V potential. The method reported 100% trapping and lysing efficiency. Despite reliable trapping and lysing of an array of single cells, the chip did not provide a way to compartmentalize single cell lysates. Thus, all extracted RNA was collected via pipette post the cell lysis step. To realize single analysis post electrical lysis, Kim et al.<sup>210</sup> integrated micro well compartmentalization, DEP immobilization, and electrical cell lysis all on one chip. The group reported 95% of 3600 wells were loaded with single cells due to DEP facilitated trapping. Following DEP immobilization, reagent exchange was done rapidly in 30 seconds via pressure driven flow, without perturbing the cell positioning. To confine lysates, the wells are physically closed by pressing a PDMS membrane on top of the wells. The group reported 100% of trapped cells were lysed simultaneously via a series of 30 V electrical pulses. Similarly, another group designed a microfluidic chip to load single cells into 30  $\mu$ m diameter wells via electroosmotic driven flow and then lyse the cells under a 30 V potential.<sup>211</sup>

Electrical approaches offer rapid cell lysis, without damaging an assay's target biomolecule, as opposed to thermal lysis. Furthermore, electrical lysis avoids target contamination contra to chemical lysis methods. Nevertheless, electrical lysis sees limited application for single cell molecular analyses. This may partly be because electrical lysis requires integration of electrodes and respective control systems on a microfluidic chip. Thus, the manufacture and operation of these chips is not trivial, and is a limiting factor to clinical adoption. Though not discussed here, optical lysis methods face a similar hurdle. Optical lysis or laser lysis is rapid, and therefore ideal for analyzing intracellular events on shorter time scales. However, laser equipment can be quite expensive and process integration complicated. The previously referenced reviews further discuss optical lysis.<sup>188-189</sup> Currently, the predominant methods of single cell lysis for molecular single cell analysis are chemical. As already discussed, this may be due to researchers' familiarity with bulk chemical lysis methods and the facile scale down to single cells.

## E. Single Cell Analysis

Up to this point, this review has discussed tissue dissociation, cell sorting, single cell compartmentalization, and single cell lysis. The next and final step in the workflow is the single cell assay. The growing interest in single cell assays has been fueled by many sources. For example, studies have shown high heterogeneity among intra tumor cancer cells,<sup>212–213</sup> spurring a debate as to whether bulk cell assays are appropriate tools for studying cancer cell genomes and transcriptomes. A plethora conventional single cell assay technologies are commonly used. Their selection is dependent on the biological application. For example, does one want to investigate the genome, transcriptome, or proteome?

Flow cytometry (FC) is one of the most well-known techniques for single cell analysis. We have already discussed a flow cytometer derivative, the FACS machine. A sample cell suspension is injected into a cone shaped cavity, filled with pressurized sheath fluid. The pressurized sheath fluid constrains the injected sample to a single laminar flow stream. This fluidic system ensures that individual cells flow past a laser. As the laser interrogates each cell, the light scatter is recorded in a direction directly opposite of the laser and a direction perpendicular to the laser incidence. These two parameters are forward scatter and side scatter; indicative of cell size and granularity. Cells labeled with fluorophores will also generate a fluorescence intensity signal.<sup>214</sup> As such, FC allows the phenotypic characterization and sorting of single cells from cell suspension. FC and FACS are instrumental tools in single cell characterization, due to their high throughput ( $10^4$  cells  $s^{-1}$ ) and multiple analyte capability.<sup>30</sup> While traditionally reserved for protein based profiling via fluorophore conjugated antibodies, new labeling strategies have enabled various FC and FACS applications. For example, FISH is typically used for detecting specific nucleic acid sequences in single cells via fluorescence microscopy. However, several groups have adopted this labeling strategy for flow cytometric RNA detection, enabling transcriptome analysis of larger sample sizes.<sup>215–216</sup> Already discussed, Lim et al.<sup>172</sup> developed a technique to sort single cell droplets via FACS on the basis of an in-droplet PCR assay, enabling genomic sequence cell characterization and sorting. FC and FACS do have some limitations as discussed previously, namely cost, large sample size requirements, and required expertise. Furthermore time-course single cells analyses are not feasible with FC or FACS.

Another technique for single cell genome and transcriptome analysis is quantitative PCR.<sup>217</sup> One challenging aspect of implementing single cell qPCR is single cell isolation. Common techniques for doing so include micromanipulation, LCM, and FACS, each with respective advantages and disadvantages. We discussed single cell qPCR in combination with inkjet-like printing for facile single cell isolation.<sup>192</sup> Microscopy is also frequently used for single cell analysis. As opposed to FACS or FC, microscopy has capability for time-course monitoring of a single cell. In combination with fluorescent labeling strategies, fluorescence microscopy allows for intracellular investigation against a variety of targets.<sup>218–220</sup> Other microscopy variants, such as confocal microscopy, allow higher resolution 3-dimensional imaging for sub single cell studies. Monks et al.<sup>221</sup> utilized confocal microscopy to study spatial distribution of surface receptors and intracellular proteins in T cells during interaction with antigen presenting cells. The study showed proteins to be spatially

segregated rather than evenly distributed. Some microscopy throughput limitations have been addressed by automating both imaging and data analysis. However, a limited field of view and difficulty discerning cell boundaries can present challenges in studying intact tissues or cultures. A variety of other conventional techniques for studying single cells are discussed elsewhere.<sup>1-3, 222-224</sup>

Interest in single cell biology is abundantly clear from the literature. However, continued discovery in this field will require new tools possessing higher sensitivity and throughput. Given the size of single cells, implementing single cell assays on microfluidic platforms is particularly attractive. Upon lysis, intracellular contents diffuse and dilute. Many target biomolecules such as RNA or proteins are present in low quantities; therefore dilution is detrimental to detection. As already discussed, microfluidic devices can be used to confine cells and their lysates into pico or femtoliter volumes, thereby prohibiting diffusion and limiting dilution. Cells, lysates, and reagents are easily confined or manipulated across these tiny volumes via predictable laminar flows. Robust microfabrication procedures can be used to tailor device dimensions to various specimens for wide applicability. Conventional single cell assay methods are frequently plagued by the laborious task of isolating and compartmentalizing a single cell, for example via LCM or micromanipulation. This issue is frequently contrasted by sample size requirements, e.g. FACS analysis offers facile cell isolation but requires large sample size. As discussed previously, microfluidic platforms are capable of high throughput cell compartmentalization even with small sample sizes.

The field of on chip single cell analysis is rapidly expanding and for further discussion, we refer the reader to several recently written reviews.<sup>38, 225-230</sup> In the next sections, recent experiments regarding on chip single cell analysis for genome, transcriptome, and proteome analysis are reviewed, particularly highlighting approaches for high throughput, multiplex analysis.

**Genome**—Sequencing technologies have significantly advanced decoding the human genome. However, these decoded genomes do not describe haplotype structure on homologous chromosomes. Haplotypes are combinations of single nucleotide polymorphisms that are inherited together. Haplotype structure has been linked to drug resistance and disease susceptibility, and thus has significant importance for human health.<sup>231-232</sup> While a variety of methods for reconstructing haplotypes have been demonstrated, many of these cannot determine their relative location along the chromosome or are low-throughput and expensive. As such, whole genome haplotyping for an individual has not been demonstrated. Fan et al.<sup>142</sup> demonstrated whole genome haplotyping via a microfluidic device. The device captures a single cell, where it is microscopically identified to be metaphase. Next, the cell is moved to a chromosome release region and the enzymatically released chromosomes are partitioned into 48 separate chambers. Chromosomes are individually amplified in the chambers and the amplified products are individually collected for downstream sequencing. This approach allows for targeted gene amplification and sequencing across all chromatids and thus determination of haplotypes. The same group utilized the microfluidic device for the first ever single sperm cell genomic analysis to characterize meiotic recombination events occurring during gametogenesis.<sup>233</sup> The device was used for loading single sperm cells into the 48 microfluidic chambers,

conducting lysis and whole genome amplification. Data from 91 single sperm cells from the same individual was used for the analysis and revealed regions where chromosome recombination occurred. The authors attributed higher throughput and reduced contamination to microfluidic implementation.

The two approaches above utilized a microfluidic platform for conducting cell compartmentalization, lysis, and DNA amplification. However, sequencing was done off chip. In contrast, Abate et al.<sup>234</sup> conducted on chip sequencing using two DNA probes, labeled with a dye pair exhibiting fluorescence resonance energy transfer (FRET). FRET is a distance dependent phenomenon, where excitation energy is transferred from a donor dye molecule to an acceptor dye molecule, thereby preventing photon emission that one would observe with a single fluorescent dye. Upon adjacently annealing to a target DNA molecule, the FRET dye pair exhibits quenching, indicating the presence of the target DNA. By varying the probe pair, various DNA targets are assayed. To conduct the analysis, the two probes are conjugated with the FRET dyes in solution, and 50  $\mu\text{m}$  diameter oil-aqueous drops are generated via microfluidic drop generator. This process is performed for various DNA probes and the drops are consolidated in one vessel. DNA for sequencing is injected on chip into each drop and incubated for one hour, followed by optical detection of the FRET signal. The system was able to distinguish instances of perfect DNA complement and single base pair mismatch.

Most single cell genomic analyses require DNA material amplification. PCR and its variants such as digital PCR (dPCR) have been implemented in microfluidic devices extensively.<sup>235–236</sup> The benefit of microfluidic implementation is usually higher throughput. For example, Heyries et al.<sup>237</sup> implemented dPCR in one million picoliter reactions on chip, representing an assay density of 440,000  $\text{cm}^{-2}$ . Despite wide implementation, PCR based amplification can introduce amplification bias. New amplification methods, such as multiple annealing and looping based amplification cycles (MALBAC) demonstrate better amplification uniformity. Yu et al.<sup>238</sup> implemented MALBAC in a microfluidic device for the parallel processing of 8 cells in less than 4 hours, enabling higher throughput and reduced contamination risk. An advantage of microfluidic DNA amplification is reduced reactor volumes, and increased surface areas. Both features result in reduced cycle time due to reduced thermal mass and increased heat transfer. Sample heating can be accomplished in several ways including resistive heaters, thermoelectric devices,<sup>238</sup> or laser irradiation. Lagally et al.<sup>239</sup> used a resistive thin film heater directly underneath the PCR chambers and reported cycle times as short as 30 seconds. Another study accomplished contactless heating via infrared irradiation<sup>240</sup>. Isothermal DNA amplification methods utilizing enzymes have also been developed and a recent review discusses their microfluidic implementation.<sup>241</sup> For further discussion of microfluidic DNA amplification, we refer the reader to additional focused reviews.<sup>242–243</sup>

The microfluidic platforms for DNA analysis discussed above typically executed only one step on chip, such as chromosome manipulation<sup>142</sup> or single cell compartmentalization and lysis.<sup>233</sup> Sequencing was performed off chip. Similarly, experiments reporting microfluidic DNA amplification usually utilize an external microscope for quantifying PCR products.<sup>236–237</sup> Integration of processing and detection is a separate challenge in

microfluidics research, and will be briefly discussed later. Nevertheless, microfluidic systems confer significant advantage over conventional technologies. The reduction in size allows for efficient heat transfer, shorter DNA amplification cycles,<sup>239</sup> and thus faster detection. Similarly, reducing reaction volume enables accurate single cell<sup>238</sup> or single molecule<sup>237</sup> DNA amplification and quantification, because the relative amount of target DNA compared to amplification reagents is increased. Finally, we have seen that massively parallel single cell analysis can be achieved on  $\text{cm}^2$  chips<sup>237</sup> for high throughput.

**Transcriptome**—Single cell gene expression analysis has been broadly applied to fields such as immunology,<sup>244</sup> neurobiology,<sup>245</sup> developmental,<sup>33</sup> and cancer biology.<sup>246</sup> Amplifying RNA is a key step in gene expression analysis and microfluidic integration has enabled single cell measurement. The low volumes achievable via microfluidics provide easier RNA detection, typically present in picogram quantities. Early microfluidic systems utilizing milliliter sized chambers for RNA analysis via RT-PCR were capable of detecting 500 starting mRNAs,<sup>247</sup> unsuitable for single cell analysis. Eventually, microfluidic systems with picoliter sized chambers and new amplification protocols were developed to detect starting RNA in the double digits, opening the door to single cell analysis.<sup>248–249</sup>

The field of microfluidic single cell gene expression analysis has experienced tremendous growth over the past decade. Early systems mostly performed on-chip RT and off qPCR, or vice versa. However, systems capable of single cell detection, high throughput, and full integration are now common. Recently, Zhu et al.<sup>250</sup> reported a droplet RT-qPCR single cell assay with integrated single cell compartmentalization, lysis, RT, qPCR, and fluorescence detection. In their work, an automated robot was used to print 2 nL single cell droplets onto a hydrophilic patterned microchip. The hydrophilic spots ensured droplet immobilization within an oil cover layer, which prevents droplet evaporation. After cell counting and thermal cell lysis is performed in 2 nL droplets, the automated robot adds 18 nL of RT reagents. After RT, 30 nL of PCR reagents are added. The significant dilution prevents RT-PCR reaction inhibition via cell lysate and buffer. The automated robot allowed for droplet generation at a rate of 20 droplets  $\text{min}^{-1}$ . The system showed repeatability, with a 2.7% relative standard deviation for fluorescent intensity across 100 droplets and a lower detection limit of 6 copies per droplet. In contrast to automated robotics, Sun et al.<sup>143</sup> reported a microfluidic device with pneumatic valves for integrated single cell compartmentalization, lysis, mRNA purification, RT, and qPCR. Purification was enabled by the use of oligo(dT) labeled beads. Similarly, Han et al.<sup>251</sup> utilized oligo(dT) functionalized magnetic beads for mRNA capture, RT, and gene amplification on a microfluidic chip. Cell lysis, however, was performed off chip. The high throughput capability of microfluidics for single cell gene expression analysis was demonstrated by White and colleagues<sup>8</sup> who built a chip for integrated cell capture, lysis, RT, and dPCR. Complementary DNA from a single cell is partitioned into a 1020 chamber dPCR array. Each chamber is 25 pL in volume. Two hundred single cells are analyzed each run, totaling to 204,000 PCR reactions, corresponding to 118,900 reactions  $\text{cm}^{-1}$ . In comparison to other methods, this study utilized single cell dPCR (in contrast to qPCR), which is better suited for quantifying lower abundance transcripts and does not require reference standards.

Microfluidic integration lends better economy of scale, and a streamlined workflow to dPCR.

The preceding discussion focused on qPCR for single cell transcriptome analysis. Despite its long history, qPCR remains an indispensable tool in genomic and transcriptomic research. However, whole transcriptome single cell RNA sequencing, developed in 2009,<sup>252</sup> has shown great potential in transcriptomic research. As we saw with qPCR; after an analytical technique is established, researchers are often interested in multiplex and high throughput implementation. That is, how can we apply the technology to thousands of cells, many target RNAs, while minimizing labor and financial cost? Single cell RNA sequencing technology is no different and microfluidics enables its high throughput application. Recently, Klein et al.<sup>200</sup> developed a microfluidic platform, termed “inDrop”, for multiplex RNA analysis of thousands of single cells simultaneously. Single cells, lysis buffer, RT reagents, and barcoded primers are encapsulated in droplets on-chip. Within each droplet, a single cell is lysed, and complementary DNA (cDNA) is synthesized using the barcoded primers. Then, all of the droplets are ruptured and the cDNA material from all single cells is combined for amplification and sequencing. The key innovation is the barcoded primers. Each droplet contains a diverse set of primers for in-depth mRNA sequencing, but each droplet’s primers are uniquely labeled with one of 147,456 barcodes. The current library of barcodes allows for 99% of 3,000 single cells to be uniquely labeled and the library can be easily expanded. Therefore, sequencing reads can be tracked back to the cell of origin. Using inDrop, the researchers processed single cells at a rate of 4,000–12,000 cells hr<sup>-1</sup>. The authors also note that this technology should be adaptable to DNA processing and integration with droplet sorting chips. However, the method did boast a low mRNA capture efficiency, making it unsuitable for detection of low abundance transcripts (< 20–50 transcripts/cell). Furthermore, the random barcoding strategy does not associate a barcode to cell type, size, location, or any other identifier.

Similarly, Macosko et al.<sup>161</sup> developed “Drop-seq”, a microfluidic droplet approach for single cell gene expression analysis. The two approaches diverge in their barcoded bead library and its preparation. Drop-seq boasts approximately 16 million unique labels compared to inDrop’s 147,456. Therefore, Drop-seq is capable of processing larger samples. However, inDrop has a higher single cell capture efficiency, enabling analysis of small samples, which are hard to come by. Furthermore, inDrop accomplishes RT in droplets while Drop-seq does so in bulk after the droplets are broken. Rotem et al.<sup>253</sup> demonstrated another microfluidic droplet based approach to labeling mRNA prior to sequencing. This method electrically coalesced two adjacent droplets, each containing either the mRNA from a single cell lysate or the unique labels. Reverse transcription reagents were injected post drop coalescence.

The microfluidic methods discussed above are addressing the current challenges in single cell gene expression analysis. One challenge is increasing sensitivity and accuracy. This is especially important for low abundance transcripts where it is difficult to differentiate signal and experimental noise. We previously discussed a microfluidic platform for single cell RT and amplification;<sup>140</sup> the authors attributed efficiency and reproducibility to low volume, microfluidic liquid handling. Another challenge is increasing throughput. Transcriptional

profiling of rare cell types, e.g. tumor cells, that are present in larger cell populations requires rare cell type enrichment and/or processing larger samples of single cells. Furthermore, in order to accurately capture stochastic effects, it is likely that many cells need to be analyzed simultaneously. Several recent droplet microfluidic platforms show great promise for increasing throughput.<sup>161, 200, 253</sup>

**Proteome**—The central dogma of biology describes the movement of hard-wired genetic information from the genome to the transcriptome, and translation to the proteome. To understand the holistic flow of information, researchers often need to study the proteome. Furthermore, given that the proteome defines the cell's functional state, its study is a high priority. Additionally, high mRNA abundance does not always correlate to high protein abundance, justifying the need for single cell proteomics. Microfluidic devices have been used for measuring single cell protein expression. Lab on a chip technology confers several advantages for single cell protein analysis; decreased sample loss and contamination, and lower detection limits. All are critical attributes for single cell protein assays because unlike DNA or RNA, proteins cannot be amplified.

Recently, several microfluidic platforms have been reported for studying single cell enzyme activity and function. For example, Xu et al.<sup>254</sup> created a microfluidic, multifunctional pipette to study alkaline phosphate (AP) activity within a single cell as a function of local cell temperature. The device is used to hydrodynamically confine a single cell in an aqueous environment, while an IR laser manipulates the environmental temperature. A confined cell was permeabilized and exposed to an enzyme substrate, fluorescein diphosphate, which undergoes reaction with AP to produce a fluorescent product. The fluorescence signal indicated enzyme activity. In contrast to traditional enzyme activity assays, this approach allows for studying enzyme activity without cell lysis or enzyme extraction. Son et al.<sup>255</sup> used a microfluidic device with a micro-patterned, antibody functionalized, hydrogel array to capture single cells and study the activity of secreted protease. The group used protease cleavable FRET peptides for detection. Dent et al.<sup>256</sup> used a microfluidic platform for profiling proteins secreted by single circulating tumor cells confined in micro wells. While the proteomic approaches discussed above measured one target protein, Hughes et al.<sup>257</sup> developed a novel microfluidic platform for multiplex single cell protein analysis. The platform is an innovative application of traditional western blotting. A 30  $\mu\text{m}$  thick polyacrylamide gel is molded with 6720, 20  $\mu\text{m}$  diameter, wells. Single cells are seeded into the wells via gravity and the cells are lysed to release intracellular proteins. Electrophoresis for each cell is achieved via an electrode that spans the entire gel. Then, antibody probes are diffused through the gel followed by imaging. The group demonstrated multiplexed measurement of 48 protein targets.

Since cascading events lead to protein production, there is growing interest in simultaneously quantifying multiple target types: proteins, metabolites, DNA, and RNA. The challenge to do so is because of the targets' chemical diversity, each requiring different preparation and detection protocols. Xue et al.<sup>258</sup> developed a "single cell barcode chip" (SCBS) for quantitative, single cell protein and metabolite measurement. The SCBS chip houses 310, 1.5 nL chambers, which are used for loading and lysing a single cell via a valve to an adjoining lysis buffer compartment. Each chamber also contains both the metabolite



and protein binding assays in a barcode format. The chip was tested on 200 single cells from a neurosphere tumor model. The test compared metabolite and protein levels, and their interactions following 24 hour drug exposure. Wu et al.<sup>259</sup> developed an automated microfluidic platform for detecting miRNAs, mRNAs, and proteins via in situ hybridization, immunostaining, and on chip flow cytometry. The entire chip is capable of testing 10 different conditions in parallel, requiring only 270 nL of reagent per condition and the protocol is performed in less than 8 hours.

Currently, microfluidic single cell protein analysis is scarce when compared to single cell analyses of the genome and transcriptome. The microfluidic platforms discussed, with one exception,<sup>257</sup> are not multiplexed. In contrast, traditional mass spectrometry proteomics allow for detection and quantification of many target proteins. Some groups have packaged traditional proteomics into a microfluidic format, but single cell analysis yields limited proteome coverage due to processing difficulties.<sup>260–261</sup> Therefore, microfluidic platforms that measure multiple targets at the single cell level are of great interest. Several recently published reviews further discuss microfluidic single cell proteomics.<sup>229, 262–263</sup>

### 3. CONCLUSIONS AND FUTURE OUTLOOK

Single cell biology is a relatively new and rapidly expanding field. Therefore it is difficult to predict the field's future focus and applications as new technologies emerge. Nevertheless, it is clear that innovative microfluidic platforms have and will continue to play an important role in both single cell biology and biology in general. What can we expect from next generation microfluidics? This review has discussed microfluidic devices used for tissue dissociation, and tissue dissociation's relative nascent compared to cell sorting applications. Therefore, it is likely that more microfluidic devices for tissue dissociation will emerge. However, one would not expect microfluidic tissue dissociation to reach the maturity of microfluidic cell sorting in the near future. This is because conventional tissue dissociation is cheap, and effective for most research applications utilizing animal tissues. An exception may be the processing of rare clinical tissue samples, which could benefit from tightly controlled microscale processing. In contrast, cell sorting was and continues to be driven by economic factors and the need to isolate rare cell populations such as CTCs and those lacking biomarkers, tasks unfit for conventional methods. Rapidly growing research and clinical applications, such as CTC based diagnostics and stem cell therapies, require cell sorting. In turn, these applications generate a necessity for facile, low cost, and high throughput cell sorting systems. These are key advantages of microfluidic devices and as such, we expect microfluidic cell sorting to continue growing. To drive adoption of microfluidic cell sorting over traditional FACS, the focus should be on increasing throughput and multiplexing capability, while simultaneously maintaining facile operation. Microfluidic cell sorters with competitive throughput ( $10^4$  cells  $s^{-1}$ ) are more frequent and further increases should promote wider adoption. As discussed, microfluidic cell sorters are being coupled to single cell genomic and proteomic assays allowing for identification, isolation, and cloning of rare cells. This may have important implications for production of biologics. Microfluidic CTC isolation is a rapidly growing derivative of cell sorting. Commercializing devices offering higher throughput for clinically relevant specimens will enable rapid and cheaper CTC isolation, propelling cancer research and personalized

therapy. Droplet microfluidics have experienced tremendous growth and have proven to be highly advantageous and flexible for single cell compartmentalization. In the future, one would expect droplet microfluidics to become a laboratory standard, enabling high throughput and multiplex drug screening, clonal selection, and whole genome sequencing.

This review discussed genomic analysis on microfluidic chips and it was observed that for sequencing experiments, the workflow is performed on chip up to DNA amplification. Sequencing is usually accomplished off chip via standard protocols. Nevertheless, one study was discussed that attempted on chip sequencing via a FRET based detection scheme. This approach however, is limited in depth. Therefore, one can anticipate that future efforts will be directed at full workflow integration, from sampling to sequencing. In fact, this has been a long sought goal in microfluidics research, the micro total analysis system ( $\mu$ TAS). Microfluidic transcriptome analysis is in a similar position. While RT-qPCR transcriptome analysis has been fully miniaturized, transcriptome wide studies via sequencing are not completely integrated. We discussed two droplet microfluidic devices, which enable very high throughput and multiplexed cDNA preparation from single cells. The massive amount of data generated by these approaches will allow mapping of complex heterogeneous tissues and will most likely uncover previously unrecognized cell types and states. However, computational biology and computer science will have to keep pace with these developments in order to decipher the data. Proteomics at the single cell level has been demonstrated in diverse formats. However, the methods highlighted in this review target only one protein or a few proteins of interest. Similarly, microfluidic packaged mass spectrometry has not attained proteome coverage equivalent to conventional mass spectrometry techniques. Therefore, future efforts in microfluidic proteomics should look to expand multiplex capabilities.

The modern era of single cell biology is particularly exciting. Technological advances in amplification, sequencing, and microfluidics have allowed us to probe the fundamental unit of life, the cell, in unprecedented ways. Single cell biology is sure to have a lasting impact in cancer, immunology, developmental biology, and stem cell research. Even though this paradigm shift in biology is relatively recent, we are curious to know what the next frontier is. Currently, researchers study single cells by removing cells from their native microenvironment and into alien buffers and tools. As such, the impact of the cell's native tissue is completely lost and the cell's behavior is irreversibly changed. It is widely accepted that cells' spatial context has profound implications. For example, tumor microenvironments are known to impact therapeutic response.<sup>264</sup> This missing dimension has not gone unnoticed. Recently published experiments describe transcriptome profiling of single cells in their native context via various methods; in situ hybridization,<sup>265</sup> photo-activated mRNA capture tags,<sup>266</sup> in situ single cell RNA sequencing<sup>267–268</sup>, spatial tissue sampling via LCM,<sup>134, 269</sup> computational approaches,<sup>270–271</sup> tomography<sup>272–273</sup> and combinatorial RNA labeling with sequential imaging.<sup>274</sup> Nevertheless, these pioneering methodologies have their limitations. Tomography is high throughput with respect to the number of cells and genes, but lacks cellular resolution. LCM, mRNA capture, and in situ sequencing achieves single cell resolution but is low throughput with respect to the number of cells. Automated imaging and in situ hybridization are higher throughput at single cell resolution but do not provide the depth of sequencing. In this sense, computational approaches integrating both

sequencing and imaging may be able to balance depth and throughput. Still, all the aforementioned techniques were demonstrated exclusively for transcriptome analysis. If the past is indicative of the future, these works only mark the beginning of a new frontier, spatial single cell omics, and innovative microfluidic instrumentation will open the floodgates.

## Acknowledgments

We gratefully acknowledge financial support from the National Institutes of Health under award U24 AI118665 (SKM) and startup funds from Northeastern University (ANK).

## Biographies

**Sanjin Hosic** earned his Bachelor's degree in Chemical Engineering from Northeastern University in 2011. From 2011 to 2013, Sanjin developed carbon nanotube (CNT) materials and CNT manufacturing techniques for next generation nonvolatile memory applications at Nantero, the first company to introduce carbon nanotubes into a semiconductor fabrication facility. From 2013 to 2014, Sanjin developed purification processes for preclinical, clinical, and commercial stage drugs and supported discovery efforts via impurity purification and scale-up at Cubist Pharmaceuticals. In 2014, Sanjin returned to Northeastern University to pursue a Ph.D in Chemical Engineering. His current research focuses on developing new micro fabricated systems for single cell analysis.

**Shashi Murthy** is a Professor of Chemical Engineering and Faculty Fellow at the Barnett Institute of Chemical and Biological Analysis at Northeastern University where he also serves as the Founding Director of the Sherman Center for Engineering Entrepreneurship Education. His current research applies microfluidic methodologies to address problems in immunology, stem cell biology, and proteomics. Murthy received his B.S. from The Johns Hopkins University, his Ph.D. from the Massachusetts Institute of Technology and performed postdoctoral research at the Harvard Medical School and Massachusetts General Hospital. He currently serves on the Features Panel of Analytical Chemistry.

**Abigail Koppes** is an Assistant Professor of Chemical Engineering at Northeastern University. Her research focuses on creating new platforms for autonomic nervous system control, with a particular focus on the impact of the enteric nervous system on the intestinal crypt-niche. Dr. Koppes received her BS and PhD from Rensselaer Polytechnic Institute and performed postdoctoral research as an NSF ADVANCE Fellow with Northeastern University, Harvard Medical School, and the Massachusetts Eye and Ear Infirmary. She is also currently a visiting scientist at the Massachusetts Institute of Technology Department of Bioengineering.

## REFERENCES

1. Blainey PC, Quake SR. *Nat Meth.* 2014; 11(1):19–21.
2. Galler K, Brautigam K, Grosse C, Popp J, Neugebauer U. *The Analyst.* 2014; 139(6):1237–1273. [PubMed: 24495980]
3. Liang J, Cai W, Sun Z. *Journal of genetics and genomics = Yi chuan xue bao.* 2014; 41(10):513–528. [PubMed: 25438696]

4. Tan DW, Jensen KB, Trotter MW, Connelly JT, Broad S, Watt FM. *Development*. 2013; 140(7):1433–1444. [PubMed: 23482486]
5. Marinov GK, Williams BA, McCue K, Schroth GP, Gertz J, Myers RM, Wold BJ. *Genome research*. 2014; 24(3):496–510. [PubMed: 24299736]
6. Wu J, Tzanakakis ES. *Biotechnol Adv*. 2013; 31(7):1047–1062. [PubMed: 24035899]
7. Carulli AJ, Samuelson LC, Schnell S. *Integr Biol (Camb)*. 2014; 6(3):243–257. [PubMed: 24480852]
8. White AK, Heyries KA, Doolin C, Vaninsberghe M, Hansen CL. *Analytical chemistry*. 2013; 85(15):7182–7190. [PubMed: 23819473]
9. Lecault V, White AK, Singhal A, Hansen CL. *Current opinion in chemical biology*. 2012; 16(3–4):381–390. [PubMed: 22525493]
10. Yin H, Marshall D. *Current opinion in biotechnology*. 2012; 23(1):110–119. [PubMed: 22133547]
11. Robin JD, Wright WE, Zou Y, Cossette SC, Lawlor MW, Gussoni E. *Journal of visualized experiments : JoVE*. 2015; (95):52307. [PubMed: 25651101]
12. Eschenhagen T, Fink C, Remmers U, Scholz H, Wattchow J, Weil J, Zimmermann W, Dohmen HH, Schafer H, Bishopric N, Wakatsuki T, Elson EL. *FASEB J*. 1997; 11(8):683–694. [PubMed: 9240969]
13. Klein D, Weisshardt P, Kleff V, Jastrow H, Jakob HG, Ergun S. *PLoS One*. 2011; 6(5):e20540. [PubMed: 21637782]
14. Uchida N, Buck DW, He D, Reitsma MJ, Masek M, Phan TV, Tsukamoto AS, Gage FH, Weissman IL. *Proc Natl Acad Sci U S A*. 2000; 97(26):14720–14725. [PubMed: 11121071]
15. Welser-Alves JV, Boroujerdi A, Milner R. *Methods in molecular biology*. 2014; 1135:345–356. [PubMed: 24510877]
16. Kohncke C, Lisewski U, Schleussner L, Gaertner C, Reichert S, Roepke TK. *Journal of visualized experiments : JoVE*. 2013; (73):e50145. [PubMed: 23524949]
17. Xu X, Colecraft HM. *Journal of visualized experiments : JoVE*. 2009; (28)
18. Voigt N, Zhou XB, Dobrev D. *Journal of visualized experiments : JoVE*. 2013; (77):e50235. [PubMed: 23852392]
19. Geem D, Medina-Contreras O, Kim W, Huang CS, Denning TL. *Journal of visualized experiments : JoVE*. 2012; (63):e4040. [PubMed: 22644046]
20. Zuk PA, Zhu M, Ashjian P, De Ugarte DA, Huang JI, Mizuno H, Alfonso ZC, Fraser JK, Benhaim P, Hedrick MH. *Molecular biology of the cell*. 2002; 13(12):4279–4295. [PubMed: 12475952]
21. Garg A, Houlihan DD, Aldridge V, Suresh S, Li KK, King AL, Sutaria R, Fear J, Bhogal RH, Lalor PF, Newsome PN. *Cytotherapy*. 2014; 16(4):545–559. [PubMed: 24629709]
22. Hattersley SM, Dyer CE, Greenman J, Haswell SJ. *Lab on a chip*. 2008; 8(11):1842–1846. [PubMed: 18941683]
23. Wallman L, Akesson E, Ceric D, Andersson PH, Day K, Hovatta O, Falci S, Laurell T, Sundstrom E. *Lab on a chip*. 2011; 11(19):3241–3248. [PubMed: 21850297]
24. Reynolds BA, Weiss S. *Dev Biol*. 1996; 175(1):1–13. [PubMed: 8608856]
25. Ziegler L, Segal-Ruder Y, Coppola G, Reis A, Geschwind D, Fainzilber M, Goldstein RS. *Experimental neurology*. 2010; 223(1):119–127. [PubMed: 19804775]
26. Lin CH, Lee DC, Chang HC, Chiu IM, Hsu CH. *Analytical chemistry*. 2013; 85(24):11920–11928. [PubMed: 24228937]
27. Qiu X, De Jesus J, Pennell M, Troiani M, Haun JB. *Lab on a chip*. 2015; 15(1):339–350. [PubMed: 25377468]
28. Marusyk A, Almendro V, Polyak K. *Nat Rev Cancer*. 2012; 12(5):323–334. [PubMed: 22513401]
29. Hulett HR, Bonner WA, Barrett J, Herzenberg LA. *Science*. 1969; 166(3906):747–749. [PubMed: 4898615]
30. Piyasena ME, Graves SW. *Lab on a chip*. 2014; 14(6):1044–1059. [PubMed: 24488050]
31. Sanchez-Freire V, Ebert AD, Kalisky T, Quake SR, Wu JC. *Nature protocols*. 2012; 7(5):829–838. [PubMed: 22481529]

32. Miltenyi S, Muller W, Weichel W, Radbruch A. *Cytometry*. 1990; 11(2):231–238. [PubMed: 1690625]
33. Treutlein B, Brownfield DG, Wu AR, Neff NF, Mantalas GL, Espinoza FH, Desai TJ, Krasnow MA, Quake SR. *Nature*. 2014; 509(7500):371–+. [PubMed: 24739965]
34. Neves RP, Raba K, Schmidt O, Honisch E, Meier-Stiegen F, Behrens B, Mohlendick B, Fehm T, Neubauer H, Klein CA, Polzer B, Sproll C, Fischer JC, Niederacher D, Stoecklein NH. *Clinical chemistry*. 2014; 60(10):1290–1297. [PubMed: 25267515]
35. Woelfle U, Breit E, Pantel K. *Journal of translational medicine*. 2005; 3(1):12. [PubMed: 15771776]
36. Xia YN, Whitesides GM. *Angew Chem Int Edit*. 1998; 37(5):550–575.
37. Shields, CWt; Reyes, CD.; Lopez, GP. *Lab on a chip*. 2015; 15(5):1230–1249. [PubMed: 25598308]
38. Thompson AM, Paguirigan AL, Kreutz JE, Radich JP, Chiu DT. *Lab on a chip*. 2014; 14(17): 3135–3142. [PubMed: 24789374]
39. Sajeesh P, Sen AK. *Microfluid Nanofluid*. 2014; 17(1):1–52.
40. Chen YC, Li P, Huang PH, Xie YL, Mai JD, Wang L, Nguyen NT, Huang TJ. *Lab on a chip*. 2014; 14(4):626–645. [PubMed: 24406985]
41. Autebert J, Coudert B, Bidard FC, Pierga JY, Descroix S, Malaquin L, Viovy JL. *Methods*. 2012; 57(3):297–307. [PubMed: 22796377]
42. Mehrishi JN, Bauer J. *Electrophoresis*. 2002; 23(13):1984–1994. [PubMed: 12210249]
43. Voldman J. *Annual review of biomedical engineering*. 2006; 8:425–454.
44. Takahashi K, Hattori A, Suzuki I, Ichiki T, Yasuda K. *Journal of nanobiotechnology*. 2004; 2(1):5. [PubMed: 15176978]
45. Guo F, Ji XH, Liu K, He RX, Zhao LB, Guo ZX, Liu W, Guo SS, Zhao XZ. *Appl Phys Lett*. 2010; 96(19)
46. Plouffe BD, Murthy SK, Lewis LH. *Reports on progress in physics*. Physical Society. 2015; 78(1): 016601.
47. Shim S, Stemke-Hale K, Noshari J, Becker FF, Gascoyne PRC. *Biomicrofluidics*. 2013; 7(1)
48. Hayes DF, Cristofanilli M, Budd GT, Ellis MJ, Stopeck A, Miller MC, Matera J, Allard WJ, Doyle GV, Terstappen LWMM. *Clin Cancer Res*. 2006; 12(14):4218–4224. [PubMed: 16857794]
49. Gascoyne PR, Noshari J, Anderson TJ, Becker FF. *Electrophoresis*. 2009; 30(8):1388–1398. [PubMed: 19306266]
50. Shim S, Stemke-Hale K, Tsimberidou AM, Noshari J, Anderson TE, Gascoyne PR. *Biomicrofluidics*. 2013; 7(1):11807. [PubMed: 24403989]
51. Moon HS, Kwon K, Kim SI, Han H, Sohn J, Lee S, Jung HI. *Lab on a chip*. 2011; 11(6):1118–1125. [PubMed: 21298159]
52. Kim U, Soh HT. *Lab on a chip*. 2009; 9(16):2313–2318. [PubMed: 19636461]
53. Yan S, Zhang J, Yuan Y, Lovrecz G, Alici G, Du H, Zhu Y, Li W. *Electrophoresis*. 2015; 36(2): 284–291. [PubMed: 25363719]
54. Xiaoxing, X.; Yobas, L. Dielectrophoretic (DEP) separation of live/dead cells on a glass slide functionalized with interdigitated 3D silicon ring microelectrodes; *Micro Electro Mechanical Systems (MEMS)*, 2014 IEEE 27th International Conference; 26–30 Jan. 2014; 2014. p. 951-954.
55. Wei Z, Li X, Zhao D, Yan H, Hu Z, Liang Z, Li Z. *Analytical chemistry*. 2014; 86(20):10215–10222. [PubMed: 25252150]
56. Jubery TZ, Srivastava SK, Dutta P. *Electrophoresis*. 2014; 35(5):691–713. [PubMed: 24338825]
57. Li M, Li WH, Zhang J, Alici G, Wen W. *J Phys D Appl Phys*. 2014; 47(6)
58. Huang C, Smith JP, Saha TN, Rhim AD, Kirby BJ. *Biomicrofluidics*. 2014; 8(4):044107. [PubMed: 25379092]
59. Smith JP, Huang C, Kirby BJ. *Biomicrofluidics*. 2015; 9(1):014116. [PubMed: 25759749]
60. Dittrich PS, Schwille P. *Analytical chemistry*. 2003; 75(21):5767–5774. [PubMed: 14588016]
61. Wu ZG, Liu AQ, Hjort K. *J Micromech Microeng*. 2007; 17(10):1992–1999.

62. Kawamata T, Yamada M, Yasuda M, Seki M. *Electrophoresis*. 2008; 29(7):1423–1430. [PubMed: 18384021]
63. Burguillos MA, Magnusson C, Nordin M, Lenshof A, Augustsson P, Hansson MJ, Elmer E, Lilja H, Brundin P, Laurell T, Deierborg T. *Plos One*. 2013; 8(5)
64. Johansson L, Nikolajeff F, Johansson S, Thorslund S. *Analytical chemistry*. 2009; 81(13):5188–5196. [PubMed: 19492800]
65. Jakobsson O, Grenvall C, Nordin M, Evander M, Laurell T. *Lab on a chip*. 2014; 14(11):1943–1950. [PubMed: 24763517]
66. Grenvall C, Magnusson C, Lilja H, Laurell PT. *Analytical chemistry*. 2015
67. Shields, CWt; Johnson, LM.; Gao, L.; Lopez, GP. *Langmuir : the ACS journal of surfaces and colloids*. 2014; 30(14):3923–3927. [PubMed: 24673242]
68. Skowronek V, Rambach RW, Schmid L, Haase K, Franke T. *Analytical chemistry*. 2013; 85(20):9955–9959. [PubMed: 24053589]
69. Li SX, Ding XY, Guo F, Chen YC, Lapsley MI, Lin SCS, Wang L, McCoy JP, Cameron CE, Huang TJ. *Analytical chemistry*. 2013; 85(11):5468–5474. [PubMed: 23647057]
70. Schmid L, Weitz DA, Franke T. *Lab on a chip*. 2014; 14(19):3710–3718. [PubMed: 25031157]
71. Yeo LY, Friend JR. *Annu Rev Fluid Mech*. 2014; 46:379–406.
72. Ding XY, Li P, Lin SCS, Stratton ZS, Nama N, Guo F, Slotcavage D, Mao XL, Shi JJ, Costanzo F, Huang TJ. *Lab on a chip*. 2013; 13(18):3626–3649. [PubMed: 23900527]
73. Ashkin A. *Physical Review Letters*. 1970; 24(4):156–159.
74. Ashkin A, Dziedzic JM, Bjorkholm JE, Chu S. *Optics letters*. 1986; 11(5):288. [PubMed: 19730608]
75. Jonas A, Zemanek P. *Electrophoresis*. 2008; 29(24):4813–4851. [PubMed: 19130566]
76. Moffitt JR, Chemla YR, Smith SB, Bustamante C. *Annu Rev Biochem*. 2008; 77:205–228. [PubMed: 18307407]
77. Hoi SK, Kim VH, Huy NM, Sow CH, Ow YS, Bettiol AA. *Biomicrofluidics*. 2010; 4(4):44111. [PubMed: 21264058]
78. Bragheri F, Minzioni P, Martinez Vazquez R, Bellini N, Paie P, Mondello C, Ramponi R, Cristiani I, Osellame R. *Lab on a chip*. 2012; 12(19):3779–3784. [PubMed: 22868483]
79. Chen Y, Wu TH, Kung YC, Teitell MA, Chiou PY. *The Analyst*. 2013; 138(24):7308–7315. [PubMed: 23844418]
80. Chen Y, Chung AJ, Wu TH, Teitell MA, Di Carlo D, Chiou PY. *Small*. 2014; 10(9):1746–1751. [PubMed: 24536017]
81. Wang X, Chen S, Kong M, Wang Z, Costa KD, Li RA, Sun D. *Lab on a chip*. 2011; 11(21):3656–3662. [PubMed: 21918752]
82. Wang C, Ye M, Cheng L, Li R, Zhu W, Shi Z, Fan C, He J, Liu J, Liu Z. *Biomaterials*. 2015; 54:55–62. [PubMed: 25907039]
83. Besant JD, Mohamadi RM, Aldridge PM, Li Y, Sargent EH, Kelley SO. *Nanoscale*. 2015; 7(14):6278–6285. [PubMed: 25784586]
84. Chen P, Huang YY, Hoshino K, Zhang JX. *Scientific reports*. 2015; 5:8745. [PubMed: 25735563]
85. Del Giudice F, Madadi H, Villone MM, D'Avino G, Cusano AM, Vecchione R, Ventre M, Maffettone PL, Netti PA. *Lab on a chip*. 2015; 15(8):1912–1922. [PubMed: 25732596]
86. Karabacak NM, Spuhler PS, Fachin F, Lim EJ, Pai V, Ozkumur E, Martel JM, Kojic N, Smith K, Chen PI, Yang J, Hwang H, Morgan B, Trautwein J, Barber TA, Stott SL, Maheswaran S, Kapur R, Haber DA, Toner M. *Nature protocols*. 2014; 9(3):694–710. [PubMed: 24577360]
87. Kim S, Han SI, Park MJ, Jeon CW, Joo YD, Choi IH, Han KH. *Analytical chemistry*. 2013; 85(5):2779–2786. [PubMed: 23384087]
88. Plouffe BD, Mahalanabis M, Lewis LH, Klapperich CM, Murthy SK. *Analytical chemistry*. 2012; 84(3):1336–1344. [PubMed: 22240089]
89. Song SH, Lee HL, Min YH, Jung HI. *Sensor Actuat B-Chem*. 2009; 141(1):210–216.
90. Lee H, Liu Y, Ham D, Westervelt RM. *Lab on a chip*. 2007; 7(3):331–337. [PubMed: 17330164]

91. Nam J, Huang H, Lim H, Lim C, Shin S. *Analytical chemistry*. 2013; 85(15):7316–7323. [PubMed: 23815099]
92. Sofla A, Cirkovic B, Hsieh A, Miklas JW, Filipovic N, Radisic M. *Biomicrofluidics*. 2013; 7(1): 14110. [PubMed: 24404002]
93. Hejazian M, Li W, Nguyen NT. *Lab on a chip*. 2015; 15(4):959–970. [PubMed: 25537573]
94. Zborowski M, Chalmers JJ. *Analytical chemistry*. 2011; 83(21):8050–8056. [PubMed: 21812408]
95. Inglis DW, Davis JA, Austin RH, Sturm JC. *Lab on a chip*. 2006; 6(5):655–658. [PubMed: 16652181]
96. Beech JP, Holm SH, Adolfsson K, Tegenfeldt JO. *Lab on a chip*. 2012; 12(6):1048–1051. [PubMed: 22327631]
97. Ranjan S, Zeming KK, Jureen R, Fisher D, Zhang Y. *Lab on a chip*. 2014; 14(21):4250–4262. [PubMed: 25209150]
98. Liu ZB, Huang F, Du JH, Shu WL, Feng HT, Xu XP, Chen Y. *Biomicrofluidics*. 2013; 7(1)
99. Holmes D, Whyte G, Bailey J, Vergara-Irigaray N, Ekpenyong A, Guck J, Duke T. *Interface Focus*. 2014; 4(6)
100. McGrath J, Jimenez M, Bridle H. *Lab on a chip*. 2014; 14(21):4139–4158. [PubMed: 25212386]
101. Di Carlo D. *Lab on a chip*. 2009; 9(21):3038–3046. [PubMed: 19823716]
102. Martel JM, Toner M. *Annual review of biomedical engineering*. 2014; 16:371–396.
103. Geislinger TM, Franke T. *Advances in colloid and interface science*. 2014; 208:161–176. [PubMed: 24674656]
104. Warkiani ME, Guan G, Luan KB, Lee WC, Bhagat AA, Chaudhuri PK, Tan DS, Lim WT, Lee SC, Chen PC, Lim CT, Han J. *Lab on a chip*. 2014; 14(1):128–137. [PubMed: 23949794]
105. Kim TH, Yoon HJ, Stella P, Nagrath S. *Biomicrofluidics*. 2014; 8(6):064117. [PubMed: 25553193]
106. Lee MG, Shin JH, Bae CY, Choi SY, Park JK. *Analytical chemistry*. 2013; 85(13):6213–6218. [PubMed: 23724953]
107. Warkiani ME, Khoo BL, Tan DS, Bhagat AA, Lim WT, Yap YS, Lee SC, Soo RA, Han J, Lim CT. *The Analyst*. 2014; 139(13):3245–3255. [PubMed: 24840240]
108. Zhou J, Giridhar PV, Kasper S, Papautsky I. *Lab on a chip*. 2013; 13(10):1919–1929. [PubMed: 23529341]
109. Ji HM, Samper V, Chen Y, Heng CK, Lim TM, Yobas L. *Biomedical microdevices*. 2008; 10(2): 251–257. [PubMed: 17914675]
110. Murthy S, Sethu P, Vunjak-Novakovic G, Toner M, Radisic M. *Biomedical microdevices*. 2006; 8(3):231–237. [PubMed: 16732418]
111. Li X, Chen W, Liu G, Lu W, Fu J. *Lab on a chip*. 2014; 14(14):2565–2575. [PubMed: 24895109]
112. Raub CB, Lee C, Kartalov E. *Sensor Actuat B-Chem*. 2015; 210:120–123.
113. Huang T, Jia CP, Jun Y, Sun WJ, Wang WT, Zhang HL, Cong H, Jing FX, Mao HJ, Jin QH, Zhang Z, Chen YJ, Li G, Mao GX, Zhao JL. *Biosensors & bioelectronics*. 2014; 51:213–218. [PubMed: 23962709]
114. McFaul SM, Lin BK, Ma HS. *Lab on a chip*. 2012; 12(13):2369–2376. [PubMed: 22517056]
115. Ito K, Sakuma S, Yokoyama Y, Arai F. *Robomech J*. 2014; 1(1):1–8.
116. Zhang P, Ren L, Zhang X, Shan Y, Wang Y, Ji Y, Yin H, Huang WE, Xu J, Ma B. *Analytical chemistry*. 2015; 87(4):2282–2289. [PubMed: 25607599]
117. Choi S, Karp JM, Karnik R. *Lab on a chip*. 2012; 12(8):1427–1430. [PubMed: 22327803]
118. Thege FI, Lannin TB, Saha TN, Tsai S, Kochman ML, Hollingsworth MA, Rhim AD, Kirby BJ. *Lab on a chip*. 2014; 14(10):1775–1784. [PubMed: 24681997]
119. Sheng WA, Ogunwobi OO, Chen T, Zhang JL, George TJ, Liu C, Fan ZH. *Lab on a chip*. 2014; 14(1):89–98. [PubMed: 24220648]
120. Wang GH, Crawford K, Turbyfield C, Lam W, Alexeev A, Sulchek T. *Lab on a chip*. 2015; 15(2):532–540. [PubMed: 25411722]
121. Zhang XR, Zhang Q, Yan T, Jiang ZY, Zhang XX, Zuo YY. *Analytical chemistry*. 2014; 86(18): 9350–9355. [PubMed: 25184988]

122. Jaitin DA, Kenigsberg E, Keren-Shaul H, Elefant N, Paul F, Zaretsky I, Mildner A, Cohen N, Jung S, Tanay A, Amit I. *Science*. 2014; 343(6172):776–779. [PubMed: 24531970]
123. Kvist T, Ahring B, Lasken R, Westermann P. *Appl Microbiol Biotechnol*. 2007; 74(4):926–935. [PubMed: 17109170]
124. Citri A, Pang ZP, Sudhof TC, Wernig M, Malenka RC. *Nature protocols*. 2012; 7(1):118–127. [PubMed: 22193304]
125. Choi JH, Ogunniyi AO, Du M, Du M, Kretschmann M, Eberhardt J, Love JC. *Biotechnology progress*. 2010; 26(3):888–895. [PubMed: 20063389]
126. Marshall IP, Blainey PC, Spormann AM, Quake SR. *Applied and environmental microbiology*. 2012; 78(24):8555–8563. [PubMed: 23023751]
127. Pamp SJ, Harrington ED, Quake SR, Relman DA, Blainey PC. *Genome research*. 2012; 22(6):1107–1119. [PubMed: 22434425]
128. Reizel Y, Chapal-Ilani N, Adar R, Itzkovitz S, Elbaz J, Maruvka YE, Segev E, Shlush LI, Dekel N, Shapiro E. *PLoS genetics*. 2011; 7(7):e1002192. [PubMed: 21829376]
129. Bonner RF, Emmert-Buck M, Cole K, Pohida T, Chuaqui R, Goldstein S, Liotta LA. *Science*. 1997; 278(5342):1481–1483. [PubMed: 9411767]
130. Domazet B, MacLennan GT, Lopez-Beltran A, Montironi R, Cheng L. *International journal of clinical and experimental pathology*. 2008; 1(6):475–488. [PubMed: 18787684]
131. Wang L, Brugge JS, Janes KA. *Proc Natl Acad Sci U S A*. 2011; 108(40):E803–E812. [PubMed: 21873240]
132. Kang Y, Norris MH, Zarzycki-Siek J, Nierman WC, Donachie SP, Hoang TT. *Genome research*. 2011; 21(6):925–935. [PubMed: 21536723]
133. Bennett RD, Ysasi AB, Belle JM, Wagner WL, Konerding MA, Blainey PC, Pyne S, Mentzer SJ. *Frontiers in oncology*. 2014; 4:260. [PubMed: 25309876]
134. Morrison JA, Box AC, McKinney MC, McLennan R, Kulesa PM. *Dev Dyn*. 2015; 244(6):774–784. [PubMed: 25809747]
135. Livesey FJ. *Briefings in functional genomics & proteomics*. 2003; 2(1):31–36. [PubMed: 15239941]
136. Marcy Y, Ishoey T, Lasken RS, Stockwell TB, Walenz BP, Halpern AL, Beeson KY, Goldberg SM, Quake SR. *PLoS genetics*. 2007; 3(9):1702–1708. [PubMed: 17892324]
137. Nilsson J, Evander M, Hammarstrom B, Laurell T. *Analytica chimica acta*. 2009; 649(2):141–157. [PubMed: 19699390]
138. Unger MA, Chou HP, Thorsen T, Scherer A, Quake SR. *Science*. 2000; 288(5463):113–116. [PubMed: 10753110]
139. Thorsen T, Maerkl SJ, Quake SR. *Science*. 2002; 298(5593):580–584. [PubMed: 12351675]
140. Streets AM, Zhang X, Cao C, Pang Y, Wu X, Xiong L, Yang L, Fu Y, Zhao L, Tang F, Huang Y. *Proc Natl Acad Sci U S A*. 2014; 111(19):7048–7053. [PubMed: 24782542]
141. Shi Q, Qin L, Wei W, Geng F, Fan R, Shin YS, Guo D, Hood L, Mischel PS, Heath JR. *Proc Natl Acad Sci U S A*. 2012; 109(2):419–424. [PubMed: 22203961]
142. Fan HC, Wang J, Potanina A, Quake SR. *Nature biotechnology*. 2011; 29(1):51–57.
143. Sun H, Olsen T, Zhu J, Tao JG, Ponnaiya B, Amundson SA, Brenner DJ, Lin Q. *Rsc Adv*. 2015; 5(7):4886–4893. [PubMed: 25883782]
144. Fabbri F, Carloni S, Zoli W, Ulivi P, Gallerani G, Fici P, Chiadini E, Passardi A, Frassinetti GL, Ragazzini A, Amadori D. *Cancer Lett*. 2013; 335(1):225–231. [PubMed: 23419522]
145. Pestrin M, Salvianti F, Galardi F, De Luca F, Turner N, Malorni L, Pazzagli M, Di Leo A, Pinzani P. *Molecular oncology*. 2015; 9(4):749–757. [PubMed: 25539732]
146. Fernandez SV, Bingham C, Fittipaldi P, Austin L, Palazzo J, Palmer G, Alpaugh K, Cristofanilli M. *Breast cancer research : BCR*. 2014; 16(5):445. [PubMed: 25307991]
147. Carpenter EL, Rader J, Ruden J, Rappaport EF, Hunter KN, Hallberg PL, Krytska K, O'Dwyer PJ, Mosse YP. *Frontiers in oncology*. 2014; 4:201. [PubMed: 25133137]
148. Kim S-H, Lee G, Park J. *Biomed. Eng. Lett*. 2013; 3(3):131–137.



149. Lindstrom S, Andersson-Svahn H. *Biochim Biophys Acta*. 2011; 1810(3):308–316. [PubMed: 20451582]
150. Bocchi M, Rambelli L, Faenza A, Giulianelli L, Pecorari N, Duqi E, Gallois JC, Guerrieri R. *Lab on a chip*. 2012; 12(17):3168–3176. [PubMed: 22767321]
151. Faenza A, Bocchi M, Duqi E, Giulianelli L, Pecorari N, Rambelli L, Guerrieri R. *Analytical chemistry*. 2013; 85(6):3446–3453. [PubMed: 23418883]
152. Lutz BR, Chen J, Schwartz DT. *Analytical chemistry*. 2006; 78(15):5429–5435. [PubMed: 16878879]
153. Lieu VH, House TA, Schwartz DT. *Analytical chemistry*. 2012; 84(4):1963–1968. [PubMed: 22276579]
154. Tanyeri M, Schroeder CM. *Nano Lett*. 2013; 13(6):2357–2364. [PubMed: 23682823]
155. Hayakawa T, Sakuma S, Fukuhara T, Yokoyama Y, Arai F. *Micromachines-Basel*. 2014; 5(3): 681–696.
156. Karimi A, Yazdi S, Ardekani AM. *Biomicrofluidics*. 2013; 7(2):21501. [PubMed: 24404005]
157. Di Carlo D, Wu LY, Lee LP. *Lab on a chip*. 2006; 6(11):1445–1449. [PubMed: 17066168]
158. Probst C, Grunberger A, Wiechert W, Kohlheyer D. *Micromachines-Basel*. 2013; 4(4):357–369.
159. Chen HY, Sun J, Wolvetang E, Cooper-White J. *Lab on a chip*. 2015; 15(4):1072–1083. [PubMed: 25519528]
160. Benavente-Babace A, Gallego-Perez D, Hansford DJ, Arana S, Perez-Lorenzo E, Mujika M. *Biosensors & bioelectronics*. 2014; 61:298–305. [PubMed: 24907537]
161. Macosko, Evan Z.; Basu, A.; Satija, R.; Nemes, J.; Shekhar, K.; Goldman, M.; Tirosh, I.; Bialas, Allison R.; Kamitaki, N.; Martersteck, Emily M.; Trombetta, John J.; Weitz, David A.; Sanes, Joshua R.; Shalek, Alex K.; Regev, A.; McCarroll, Steven A. *Cell*. 2015; 161(5):1202–1214. [PubMed: 26000488]
162. Guan A, Shenoy A, Smith R, Li Z. *Biomicrofluidics*. 2015; 9(2):024103. [PubMed: 25825618]
163. Bell L, Seshia A, Lando D, Laue E, Palayret M, Lee SF, Klenerman D. *Sensor Actuat B-Chem*. 2014; 192:36–41.
164. Deng B, Li XF, Chen DY, You LD, Wang JB, Chen J. *Sci World J*. 2014
165. Espulgar W, Yamaguchi Y, Aoki W, Mita D, Saito M, Lee J-K, Tamiya E. *Sensors and Actuators B: Chemical*. 2015; 207:43–50. Part A (0).
166. Jin D, Deng B, Li JX, Cai W, Tu L, Chen J, Wu Q, Wang WH. *Biomicrofluidics*. 2015; 9(1): 014101. [PubMed: 25610513]
167. de Wagenaar B, Berendsen JTW, Bomer JG, Olthuis W, van den Berg A, Segerink LI. *Lab on a chip*. 2015; 15(5):1294–1301. [PubMed: 25578490]
168. Utada AS, Lorenceau E, Link DR, Kaplan PD, Stone HA, Weitz DA. *Science*. 2005; 308(5721): 537–541. [PubMed: 15845850]
169. Zinchenko A, Devenish SRA, Kintsos B, Colin PY, Fischechner M, Hollfelder F. *Analytical chemistry*. 2014; 86(5):2526–2533. [PubMed: 24517505]
170. Kiss MM, Ortoleva-Donnelly L, Beer NR, Warner J, Bailey CG, Colston BW, Rothberg JM, Link DR, Leamon JH. *Analytical chemistry*. 2008; 80(23):8975–8981. [PubMed: 19551929]
171. Edd JF, Di Carlo D, Humphry KJ, Koster S, Irimia D, Weitz DA, Toner M. *Lab on a chip*. 2008; 8(8):1262–1264. [PubMed: 18651066]
172. Lim SW, Tran TM, Abate AR. *Plos One*. 2015; 10(1)
173. He MY, Edgar JS, Jeffries GDM, Lorenz RM, Shelby JP, Chiu DT. *Analytical chemistry*. 2005; 77(6):1539–1544. [PubMed: 15762555]
174. Ramji R, Wang M, Bhagat AAS, Weng DTS, Thakor NV, Lim CT, Chen CH. *Biomicrofluidics*. 2014; 8(3)
175. Kemna EWM, Schoeman RM, Wolbers F, Vermes I, Weitz DA, van den Berg A. *Lab on a chip*. 2012; 12(16):2881–2887. [PubMed: 22688131]
176. Jing TY, Ramji R, Warkiani ME, Han J, Lim CT, Chen CH. *Biosensors & bioelectronics*. 2015; 66:19–23. [PubMed: 25460876]

177. Schoeman RM, Kemna EW, Wolbers F, van den Berg A. *Electrophoresis*. 2014; 35(2–3):385–392. [PubMed: 23856757]
178. Tran TM, Lan F, Thompson CS, Abate AR. *J Phys D Appl Phys*. 2013; 46(11)
179. Guo MT, Rotem A, Heyman JA, Weitz DA. *Lab on a chip*. 2012; 12(12):2146–2155. [PubMed: 22318506]
180. Zhou J, Bruns MA, Tiedje JM. *Applied and environmental microbiology*. 1996; 62(2):316–322. [PubMed: 8593035]
181. Middelberg AP. *Biotechnol Adv*. 1995; 13(3):491–551. [PubMed: 14536098]
182. Gunerken E, D’Hondt E, Eppink MH, Garcia-Gonzalez L, Elst K, Wijffels RH. *Biotechnol Adv*. 2015; 33(2):243–260. [PubMed: 25656098]
183. Cheow LF, Sarkar A, Kolitz S, Lauffenburger D, Han J. *Analytical chemistry*. 2014; 86(15):7455–7462. [PubMed: 25025773]
184. Zhang H, Jin WR. *Electrophoresis*. 2004; 25(7–8):1090–1095. [PubMed: 15095451]
185. Kim SA, Yoon JA, Kang MJ, Choi YM, Chae SJ, Moon SY. *Fertil Steril*. 2009; 92(2):814–818. [PubMed: 18706553]
186. Han L, Zi X, Garmire LX, Wu Y, Weissman SM, Pan X, Fan R. *Scientific reports*. 2014; 4:6485. [PubMed: 25255798]
187. Shoemaker GK, Lorieau J, Lau LH, Gillmor CS, Palcic MM. *Analytical chemistry*. 2005; 77(10):3132–3137. [PubMed: 15889901]
188. Nan L, Jiang Z, Wei X. *Lab on a chip*. 2014; 14(6):1060–1073. [PubMed: 24480982]
189. Brown RB, Audet J. *Journal of the Royal Society, Interface / the Royal Society*. 2008; (5 Suppl 2):S131–S138.
190. Kim BC, Moraes C, Huang J, Matsuoka T, Thouless MD, Takayama S. *Small*. 2014; 10(19):4020–4029. [PubMed: 24942855]
191. Hoefemann H, Wadle S, Bakhtina N, Kondrashov V, Wangler N, Zengerle R. *Sensor Actuat B-Chem*. 2012; 168:442–445.
192. Stumpf F, Schoendube J, Gross A, Rath C, Niekrawietz S, Koltay P, Roth G. *Biosensors & bioelectronics*. 2015; 69:301–306. [PubMed: 25771302]
193. Gong YA, Ogunniyi AO, Love JC. *Lab on a chip*. 2010; 10(18):2334–2337. [PubMed: 20686711]
194. *Systems Biomedicine: Concepts and Perspectives*. 2010:1–439.
195. Leung K, Zahn H, Leaver T, Konwar KM, Hanson NW, Pagé AP, Lo C-C, Chain PS, Hallam SJ, Hansen CL. *Proceedings of the National Academy of Sciences*. 2012; 109(20):7665–7670.
196. Noelker C, Morel L, Osterloh A, Alvarez-Fischer D, Lescot T, Breloer M, Gold M, Oertel WH, Henze C, Michel PP, Dodel RC, Lu L, Hirsch EC, Hunot S, Hartmann A. *J Neuroinflammation*. 2014; 11:86. [PubMed: 24886419]
197. Debnath A, Parsonage D, Andrade RM, He C, Cobo ER, Hirata K, Chen S, Garcia-Rivera G, Orozco E, Martinez MB, Gunatilleke SS, Barrios AM, Arkin MR, Poole LB, McKerrow JH, Reed SL. *Nat Med*. 2012; 18(6):956–960. [PubMed: 22610278]
198. Yu Z, Gao YQ, Feng H, Lee YY, Li MS, Tian Y, Go MY, Yu DY, Cheung YS, Lai PB, Yu J, Wong VW, Sung JJ, Chan HL, Cheng AS. *Gut*. 2014; 63(11):1793–1804. [PubMed: 24440987]
199. DeKosky BJ, Kojima T, Rodin A, Charab W, Ippolito GC, Ellington AD, Georgiou G. *Nat Med*. 2015; 21(1):86–91. [PubMed: 25501908]
200. Klein AM, Mazutis L, Akartuna I, Tallapragada N, Veres A, Li V, Peshkin L, Weitz DA, Kirschner MW. *Cell*. 2015; 161(5):1187–1201. [PubMed: 26000487]
201. Rival A, Jary D, Delattre C, Fouillet Y, Castellan G, Bellemin-Comte A, Gidrol X. *Lab on a chip*. 2014; 14(19):3739–3749. [PubMed: 25080028]
202. Sarkar A, Kolitz S, Lauffenburger DA, Han J. *Nat Commun*. 2014; 5:3421. [PubMed: 24594667]
203. Tsong TY. *Biophys J*. 1991; 60(2):297–306. [PubMed: 1912274]
204. Sersa G, Miklavcic D, Cemazar M, Rudolf Z, Pucihar G, Snoj M. *Eur J Surg Oncol*. 2008; 34(2):232–240. [PubMed: 17614247]
205. Lee S-W, Tai Y-C. *Sensors and Actuators A: Physical*. 1999; 73(1–2):74–79.
206. Lu H, Schmidt MA, Jensen KF. *Lab on a chip*. 2005; 5(1):23–29. [PubMed: 15616736]

207. Mellors JS, Jorabchi K, Smith LM, Ramsey JM. *Analytical chemistry*. 2010; 82(3):967–973. [PubMed: 20058879]
208. Young CW, Hsieh JL, Ay C. *Sensors (Basel)*. 2012; 12(3):2400–2413. [PubMed: 22736957]
209. Bahi MM, Tsaloglou MN, Mowlem M, Morgan H. *Journal of the Royal Society, Interface / the Royal Society*. 2011; 8(57):601–608.
210. Kim SH, Yamamoto T, Fourmy D, Fujii T. *Small*. 2011; 7(22):3239–3247. [PubMed: 21932278]
211. Jen CP, Amstislavskaya TG, Liu YH, Hsiao JH, Chen YH. *Sensors (Basel)*. 2012; 12(6):6967–6977. [PubMed: 22969331]
212. Park SY, Gonen M, Kim HJ, Michor F, Polyak K. *J Clin Invest*. 2010; 120(2):636–644. [PubMed: 20101094]
213. Torres L, Ribeiro FR, Pandis N, Andersen JA, Heim S, Teixeira MR. *Breast Cancer Res Tr*. 2007; 102(2):143–155.
214. King D. *MLO Med Lab Obs*. 2007; 39(6):26. [PubMed: 17691703]
215. Porichis F, Hart MG, Griesbeck M, Everett HL, Hassan M, Baxter AE, Lindqvist M, Miller SM, Soghoian DZ, Kavanagh DG, Reynolds S, Norris B, Mordecai SK, Nguyen Q, Lai CF, Kaufmann DE. *Nature Communications*. 2014:5.
216. Wu MY, Piccini ME, Singh AK. *In Situ Hybridization Protocols*, 4th Edition. 2014; 1211:245–260.
217. Ståhlberg A, Kubista M. *Expert Review of Molecular Diagnostics*. 2014; 14(3):323–331. [PubMed: 24649819]
218. Muzzey D, van Oudenaarden A. *Annu Rev Cell Dev Biol*. 2009; 25:301–327. [PubMed: 19575655]
219. Meyer P, Dworkin J. *Res Microbiol*. 2007; 158(3):187–194. [PubMed: 17349779]
220. Kentner D, Sourjik V. *Annu Rev Microbiol*. 2010; 64:373–390. [PubMed: 20528689]
221. Monks CR, Freiberg BA, Kupfer H, Sciaky N, Kupfer A. *Nature*. 1998; 395(6697):82–86. [PubMed: 9738502]
222. Sandberg R. *Nature methods*. 2014; 11(1):22–24. [PubMed: 24524133]
223. Kolodziejczyk, Aleksandra A.; Kim, JK.; Svensson, V.; Marioni, John C.; Teichmann, Sarah A. *Molecular Cell*. 2015; 58(4):610–620. [PubMed: 26000846]
224. Wang Y, Navin Nicholas E. *Molecular Cell*. 2015; 58(4):598–609. [PubMed: 26000845]
225. Kulkarni RP, Che J, Dhar M, Di Carlo D. *Lab on a chip*. 2014; 14(19):3663–3667.
226. Streets AM, Huang Y. *Current opinion in biotechnology*. 2014; 25:69–77. [PubMed: 24484883]
227. Tsioris K, Torres AJ, Douce TB, Love JC. *Annual review of chemical and biomolecular engineering*. 2014; 5:455–477.
228. Weaver WM, Tseng P, Kunze A, Masaeli M, Chung AJ, Dudani JS, Kittur H, Kulkarni RP, Di Carlo D. *Current opinion in biotechnology*. 2014; 25:114–123. [PubMed: 24484889]
229. Yu J, Zhou J, Sutherland A, Wei W, Shin YS, Xue M, Heath JR. *Annual review of analytical chemistry*. 2014; 7:275–295.
230. Vasdekis AE, Stephanopoulos G. *Metabolic engineering*. 2015; 27:115–135. [PubMed: 25448400]
231. de Bakker PIW, McVean G, Sabeti PC, Miretti MM, Green T, Marchini J, Ke X, Monsuur AJ, Whittaker P, Delgado M, Morrison J, Richardson A, Walsh EC, Gao X, Galver L, Hart J, Hafler DA, Pericak-Vance M, Todd JA, Daly MJ, Trowsdale J, Wijmenga C, Vyse TJ, Beck S, Murray SS, Carrington M, Gregory S, Deloukas P, Rioux JD. *Nat Genet*. 2006; 38(10):1166–1172. [PubMed: 16998491]
232. Stewart CA, Horton R, Allcock RJN, Ashurst JL, Atrazhev AM, Coggill P, Dunham I, Forbes S, Halls K, Howson JMM, Humphray SJ, Hunt S, Mungall AJ, Osoegawa K, Palmer S, Roberts AN, Rogers J, Sims S, Wang Y, Wilming LG, Elliott JF, de Jong PJ, Sawcer S, Todd JA, Trowsdale J, Beck S. *Genome research*. 2004; 14(6):1176–1187. [PubMed: 15140828]
233. Wang J, Fan HC, Behr B, Quake SR. *Cell*. 2012; 150(2):402–412. [PubMed: 22817899]
234. Abate AR, Hung T, Sperling RA, Mary P, Rotem A, Agresti JJ, Weiner MA, Weitz DA. *Lab on a chip*. 2013; 13(24):4864–4869. [PubMed: 24185402]

235. Sundberg SO, Wittwer CT, Gao C, Gale BK. *Analytical chemistry*. 2010; 82(4):1546–1550. [PubMed: 20085301]
236. Shen F, Du W, Kreutz JE, Fok A, Ismagilov RF. *Lab on a chip*. 2010; 10(20):2666–2672. [PubMed: 20596567]
237. Heyries KA, Tropini C, Vaninsberghe M, Doolin C, Petriv OI, Singhal A, Leung K, Hughesman CB, Hansen CL. *Nature methods*. 2011; 8(8):649–651. [PubMed: 21725299]
238. Yu Z, Lu S, Huang Y. *Analytical chemistry*. 2014; 86(19):9386–9390. [PubMed: 25233049]
239. Lagally ET, Medintz I, Mathies RA. *Analytical chemistry*. 2001; 73(3):565–570. [PubMed: 11217764]
240. Le Roux D, Root BE, Reedy CR, Hickey JA, Scott ON, Bienvenue JM, Landers JP, Chassagne L, de Mazancourt P. *Analytical chemistry*. 2014; 86(16):8192–8199. [PubMed: 25091472]
241. Vicky T, ouml;ger\* , Katja N, G C, auml;rtig; Dirk K. 2015; (3) 6.
242. Zhang Y, Ozdemir P. *Analytica chimica acta*. 2009; 638(2):115–125. [PubMed: 19327449]
243. Asiello PJ, Baeumner AJ. *Lab on a chip*. 2011; 11(8):1420–1430. [PubMed: 21387067]
244. Mahata B, Zhang X, Kolodziejczyk AA, Proserpio V, Haim-Vilmovsky L, Taylor AE, Hebenstreit D, Dingler FA, Moignard V, Gottgens B, Arlt W, McKenzie AN, Teichmann SA. *Cell Rep*. 2014; 7(4):1130–1142. [PubMed: 24813893]
245. Usoskin D, Furlan A, Islam S, Abdo H, Lonnerberg P, Lou D, Hjerling-Leffler J, Haeggstrom J, Kharchenko O, Kharchenko PV, Linnarsson S, Ernfors P. *Nat Neurosci*. 2015; 18(1):145–153. [PubMed: 25420068]
246. Aceto N, Bardia A, Miyamoto DT, Donaldson MC, Wittner BS, Spencer JA, Yu M, Pely A, Engstrom A, Zhu H, Brannigan BW, Kapur R, Stott SL, Shioda T, Ramaswamy S, Ting DT, Lin CP, Toner M, Haber DA, Maheswaran S. *Cell*. 2014; 158(5):1110–1122. [PubMed: 25171411]
247. Anderson RC, Su X, Bogdan GJ, Fenton J. *Nucleic Acids Res*. 2000; 28(12):E60. [PubMed: 10871383]
248. Toriello NM, Liu CN, Mathies RA. *Analytical chemistry*. 2006; 78(23):7997–8003. [PubMed: 17134132]
249. Marcus JS, Anderson WF, Quake SR. *Analytical chemistry*. 2006; 78(3):956–958. [PubMed: 16448074]
250. Zhu Y, Zhang Y-X, Liu W-W, Ma Y, Fang Q, Yao B. *Sci. Rep*. 2015; 5
251. Han N, Shin JH, Han KH. *Rsc Adv*. 2014; 4(18):9160–9165.
252. Tang F, Barbacioru C, Wang Y, Nordman E, Lee C, Xu N, Wang X, Bodeau J, Tuch BB, Siddiqui A, Lao K, Surani MA. *Nature methods*. 2009; 6(5):377–382. [PubMed: 19349980]
253. Rotem A, Ram O, Shores N, Sperling RA, Schnall-Levin M, Zhang H, Basu A, Bernstein BE, Weitz DA. *PLoS ONE*. 2015; 10(5):e0116328. [PubMed: 26000628]
254. Xu S, Ainla A, Jardemark K, Jesorka A, Jeffries GD. *Analytical chemistry*. 2015; 87(1):381–387. [PubMed: 25457650]
255. Son KJ, Shin DS, Kwa T, You J, Gao YD, Revzin A. *Lab on a chip*. 2015; 15(3):637–641. [PubMed: 25421651]
256. Deng Y, Zhang Y, Sun S, Wang Z, Wang M, Yu B, Czajkowsky DM, Liu B, Li Y, Wei W, Shi Q. *Sci. Rep*. 2014:4.
257. Hughes AJ, Spelke DP, Xu Z, Kang CC, Schaffer DV, Herr AE. *Nature methods*. 2014; 11(7):749–755. [PubMed: 24880876]
258. Xue M, Wei W, Su YP, Kirn J, Shin YS, Mai WX, Nathanson DA, Heath JR. *J Am Chem Soc*. 2015; 137(12):4066–4069. [PubMed: 25789560]
259. Wu M, Singh AK. *Journal of laboratory automation*. 2014; 19(6):587–592. [PubMed: 25027027]
260. He X, Chen Q, Zhang Y, Lin J-M. *TrAC Trends in Analytical Chemistry*. 2014; 53(0):84–97.
261. Feng X, Liu B-F, Li J, Liu X. *Mass Spectrometry Reviews*. 2014 n/a-n/a.
262. Liu Y, Singh AK. *Journal of laboratory automation*. 2013; 18(6):446–454. [PubMed: 23821679]
263. Miller, E. *Proteomics in Microfluidic Devices*. In: Li, D., editor. *Encyclopedia of Microfluidics and Nanofluidics*. New York: Springer; 2015. p. 2884-2895.
264. Junttila MR, de Sauvage FJ. *Nature*. 2013; 501(7467):346–354. [PubMed: 24048067]

265. Huang Y, Yu X, Sun N, Qiao N, Cao Y, Boyd-Kirkup JD, Shen Q, Han JD. *Genome research*. 2015; 25(4):570–581. [PubMed: 25575549]
266. Lovatt D, Ruble BK, Lee J, Dueck H, Kim TK, Fisher S, Francis C, Spaethling JM, Wolf JA, Grady MS, Ulyanova AV, Yeldell SB, Gripenburg JC, Buckley PT, Kim J, Sul JY, Dmochowski JJ, Eberwine J. *Nature methods*. 2014; 11(2):190–196. [PubMed: 24412976]
267. Lee JH, Daugharthy ER, Scheiman J, Kalhor R, Yang JL, Ferrante TC, Terry R, Jeanty SS, Li C, Amamoto R, Peters DT, Turczyk BM, Marblestone AH, Inverso SA, Bernard A, Mali P, Rios X, Aach J, Church GM. *Science*. 2014; 343(6177):1360–1363. [PubMed: 24578530]
268. Ke R, Mignardi M, Pacureanu A, Svedlund J, Botling J, Wahlby C, Nilsson M. *Nature methods*. 2013; 10(9):857–860. [PubMed: 23852452]
269. Zechel S, Zajac P, Lonnerberg P, Ibanez CF, Linnarsson S. *Genome Biol*. 2014; 15(10):486. [PubMed: 25344199]
270. Achim K, Pettit JB, Saraiva LR, Gavriouchkina D, Larsson T, Arendt D, Marioni JC. *Nature biotechnology*. 2015; 33(5):503–509.
271. Satija R, Farrell JA, Gennert D, Schier AF, Regev A. *Nature biotechnology*. 2015; 33(5):495–502.
272. Junker JP, Noel ES, Guryev V, Peterson KA, Shah G, Huisken J, McMahon AP, Berezikov E, Bakkers J, van Oudenaarden A. *Cell*. 2014; 159(3):662–675. [PubMed: 25417113]
273. Combs PA, Eisen MB. *PLoS One*. 2013; 8(8):e71820. [PubMed: 23951250]
274. Chen KH, Boettiger AN, Moffitt JR, Wang S, Zhuang X. *Science*. 2015; 348(6233):aaa6090. [PubMed: 25858977]

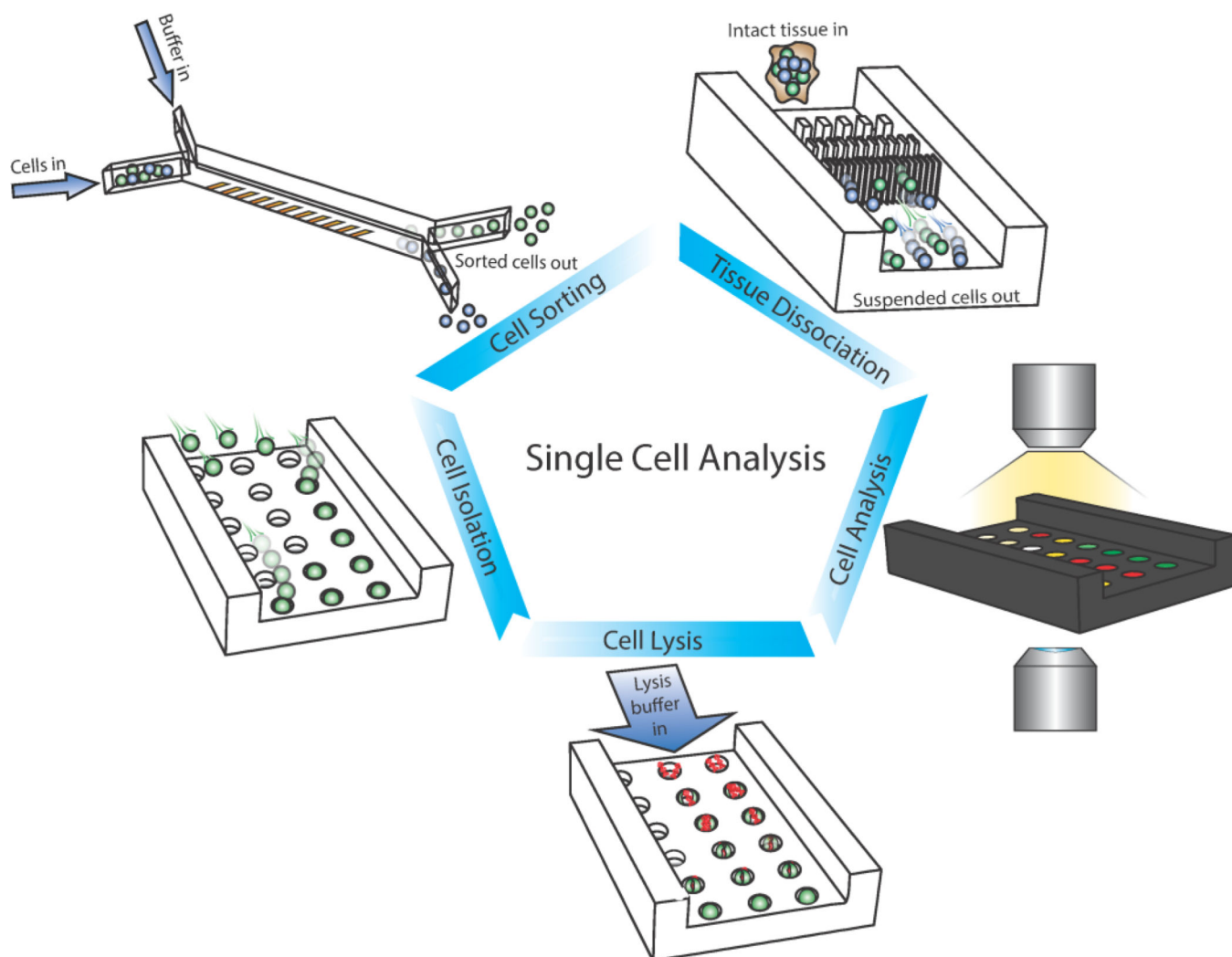


**Figure 1.**  
Sample preparation workflow for single cell analysis.

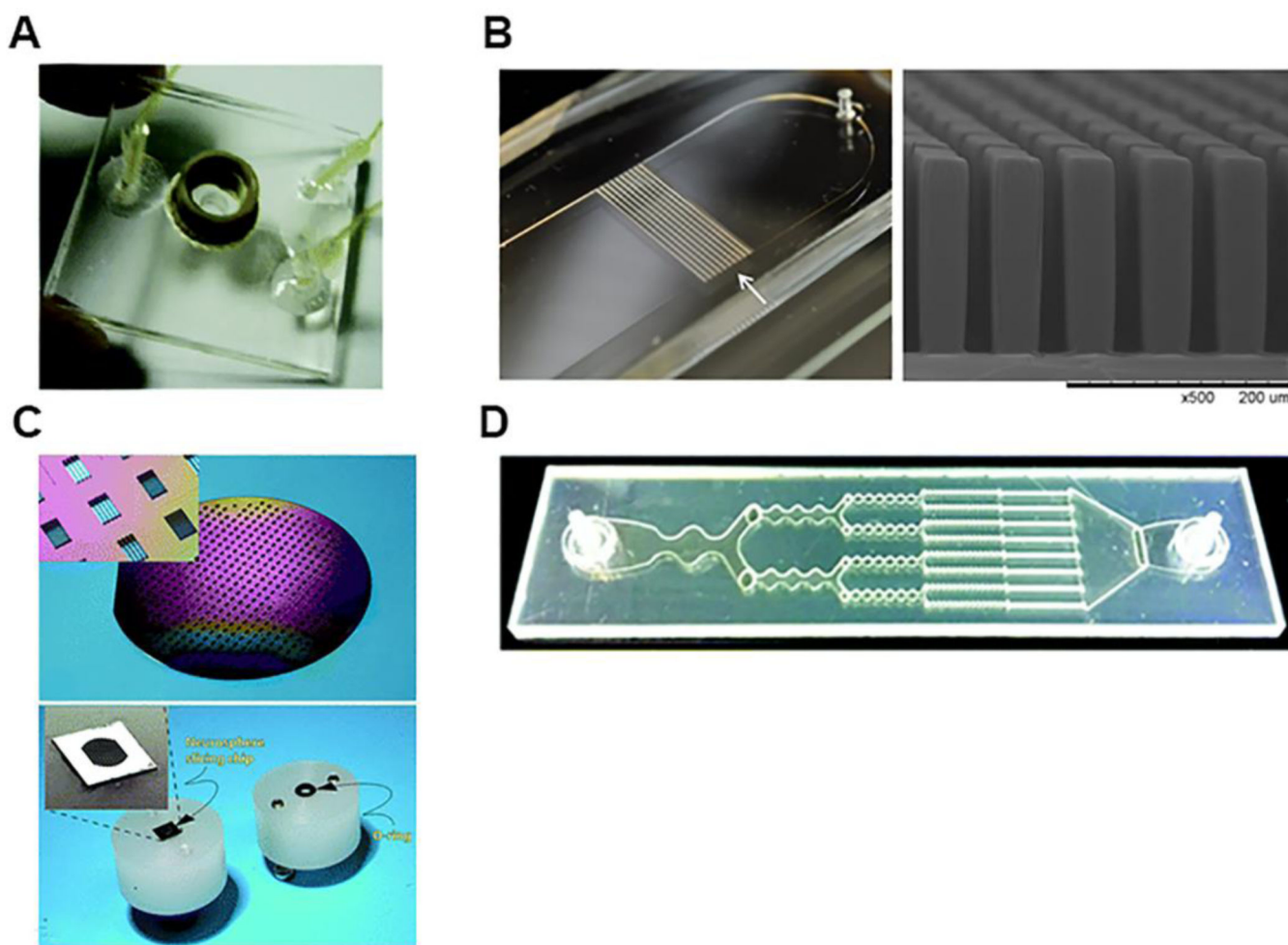


**Figure 2.**

Micro fabricated devices for tissue dissociation. (A) A photograph of a chip for whole tissue culture and dissociation showing the open tissue chamber and inlets and outlets. Reproduced from Hattersley, S. M.; Dyer, C. E.; Greenman, J.; Haswell, S. J. *Lab on a chip* 2008, 8 (11), 1842-6 (ref 22), with permission of the Royal Society of Chemistry. (B) Left photograph: the single channel “ $\mu$ -CDC” chip fabricated via soft lithography and PDMS. Right scanning electron micrograph: the micro fabricated pillars. Neurospheres traveling through the micro pillar array are mechanically dissociated into single cells. Reproduced from Lin, C. H.; Lee, D. C.; Chang, H. C.; Chiu, I. M.; Hsu, C. H. *Analytical chemistry* 2013, 85 (24), 11920-8 (ref 26). Copyright 2013 American Chemical Society. (C) Top photograph: micro fabricated 3” silicon wafer. The photograph inset shows the dissociating grids prior to wafer dicing. Bottom photograph: individual micro grids are assembled into the device adapter prior to use for cell dissociation. Reproduced from Wallman, L.; Akesson, E.; Ceric, D.; Andersson, P. H.; Day, K.; Hovatta, O.; Falci, S.; Laurell, T.; Sundstrom, E. *Lab on a chip* 2011, 11 (19), 3241-8 (ref 23), with permission of the Royal Society of Chemistry. (D) Photograph of fabricated device for dissociating small tumor tissue via alternating constriction and expansion regions. Reproduced from Qiu, X.; De Jesus, J.; Pennell, M.; Troiani, M.; Haun,

J. B. Lab on a chip 2015, 15 (1), 339-50 (ref 27), with permission of the Royal Society of Chemistry.

Author Manuscript

Author Manuscript

Author Manuscript

Author Manuscript



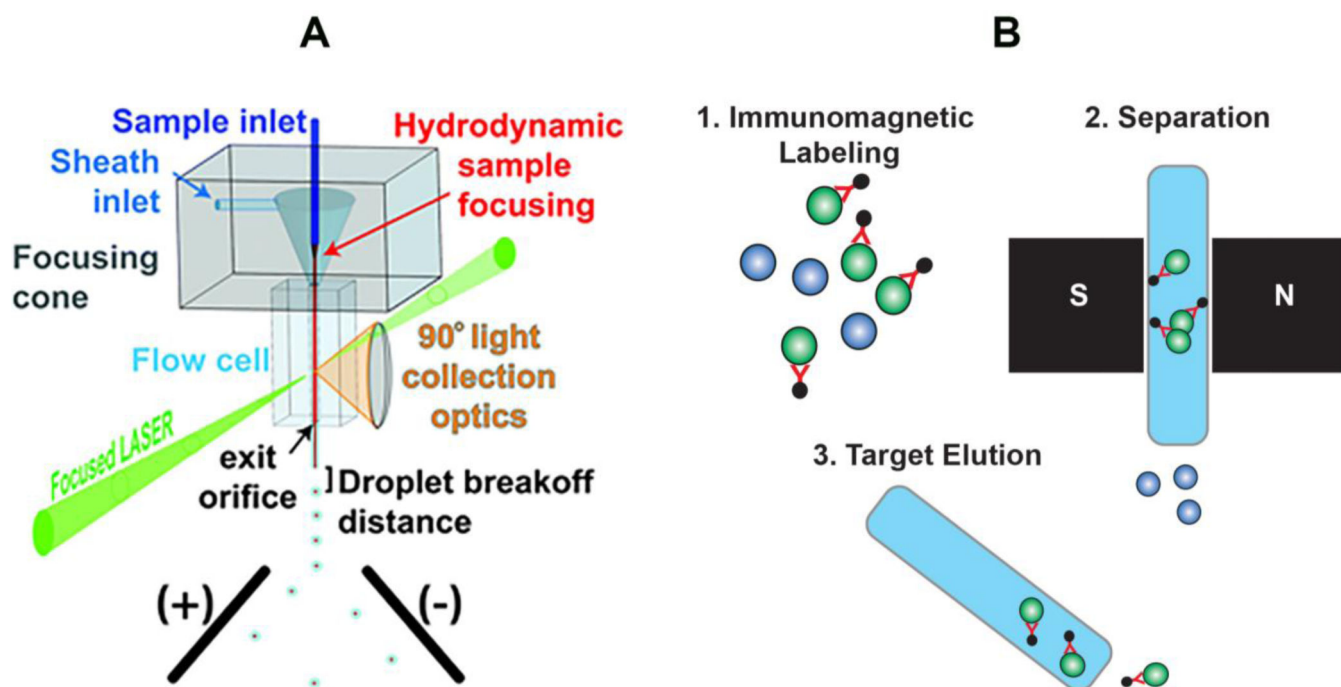


**Figure 3.** Conventional cell sorting techniques. (A) A schematic diagram of a FACS instrument. Sheath flow focuses cells which are then interrogated by a laser and given a specific charge based upon the laser signal. Cells are then deflected into containers via an electric field. Reproduced from Piyasena, M. E.; Graves, S. W. *Lab on a chip* 2014, 14 (6), 1044-59 (ref 30), with permission of the Royal Society of Chemistry. (B) A diagram schematic of MACS based cell separation. Target cells are labeled with magnetic beads and separated from non-target cells via a magnetic field.

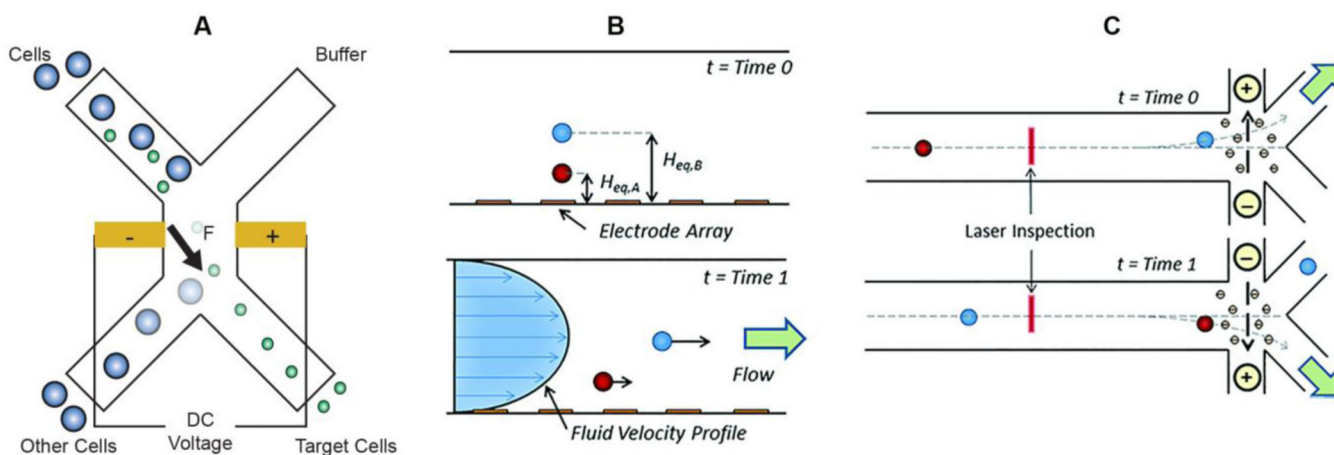


**Figure 4.**

Electrically based microscale cell separation techniques. (A) A schematic of EP cell separation. A positively charged electrode induces a Coulomb force on negatively charged cells, resulting in a net force toward the positive electrode. Cells are separated by their net charge. (B) A schematic of DEP-FFF. An upward DEP force and downward gravity force positions different cell types at distinct regions of a parabolic velocity profile, resulting in discrete retention times for each cell type. Reproduced from Shields, C. W.; Reyes, C. D.; Lopez, G. P. *Lab on a Chip* 2015, 15 (5), 1230-49 (ref 37), with permission of the Royal Society of Chemistry. (C) A schematic of EOF cell separation. Solvated negatively charged ions migrate toward the positive electrode, inducing secondary fluid movement and thereby cell separation. The electrode configuration is controlled by the signal generated via upstream laser interrogation. Reproduced from Shields, C. W. t.; Reyes, C. D.; Lopez, G. P. *Lab on a Chip* 2015, 15 (5), 1230-49 (ref 37), with permission of the Royal Society of Chemistry.

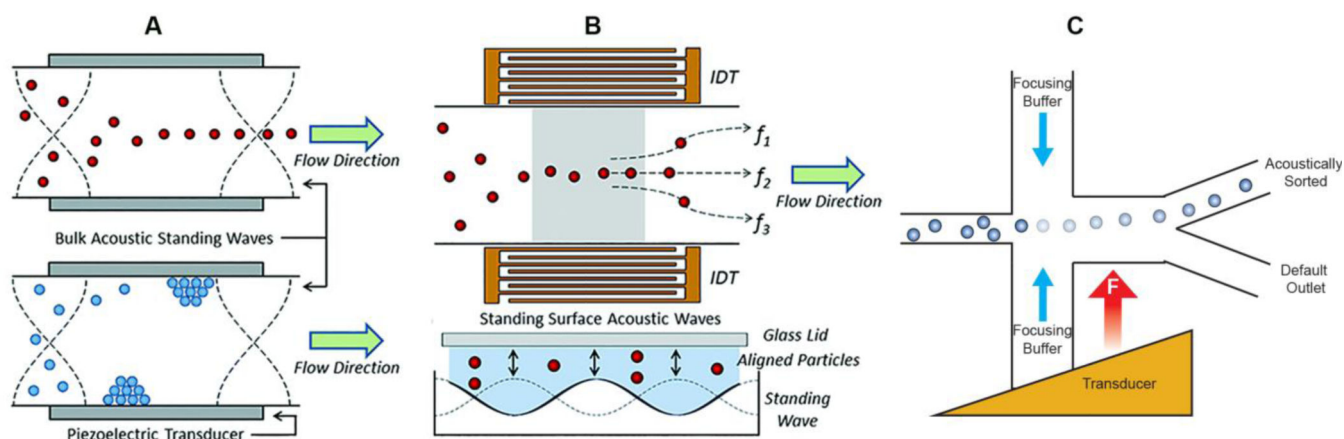


**Figure 5.**

Acoustic based microscale cell separation techniques. (A) A schematic of acoustic cell separation via bulk standing waves. Cells migrate to the node or antinode depending on their acoustic contrast factor. Reproduced from Shields, C. W.; Reyes, C. D.; Lopez, G. P. *Lab on a chip* 2015, 15 (5), 1230-49 (ref 37), with permission of the Royal Society of Chemistry. (B) A schematic of acoustic cell separation via standing surface waves. The acoustic waves, generated by interdigitated electrodes, position cells at distinct streamlines and the cells are separated via bifurcating outlets. Reproduced from Shields, C. W. t.; Reyes, C. D.; Lopez, G. P. *Lab on a chip* 2015, 15 (5), 1230-49 (ref 37), with permission of the Royal Society of Chemistry. (C) A schematic of acoustic cell separation via traveling waves. The wave is generated at a distance from the channel via a transducer and the acoustic wave travels in a direction perpendicular to the fluid flow, thereby deflecting cells traveling along the fluid streamlines into an appropriate outlet channel.

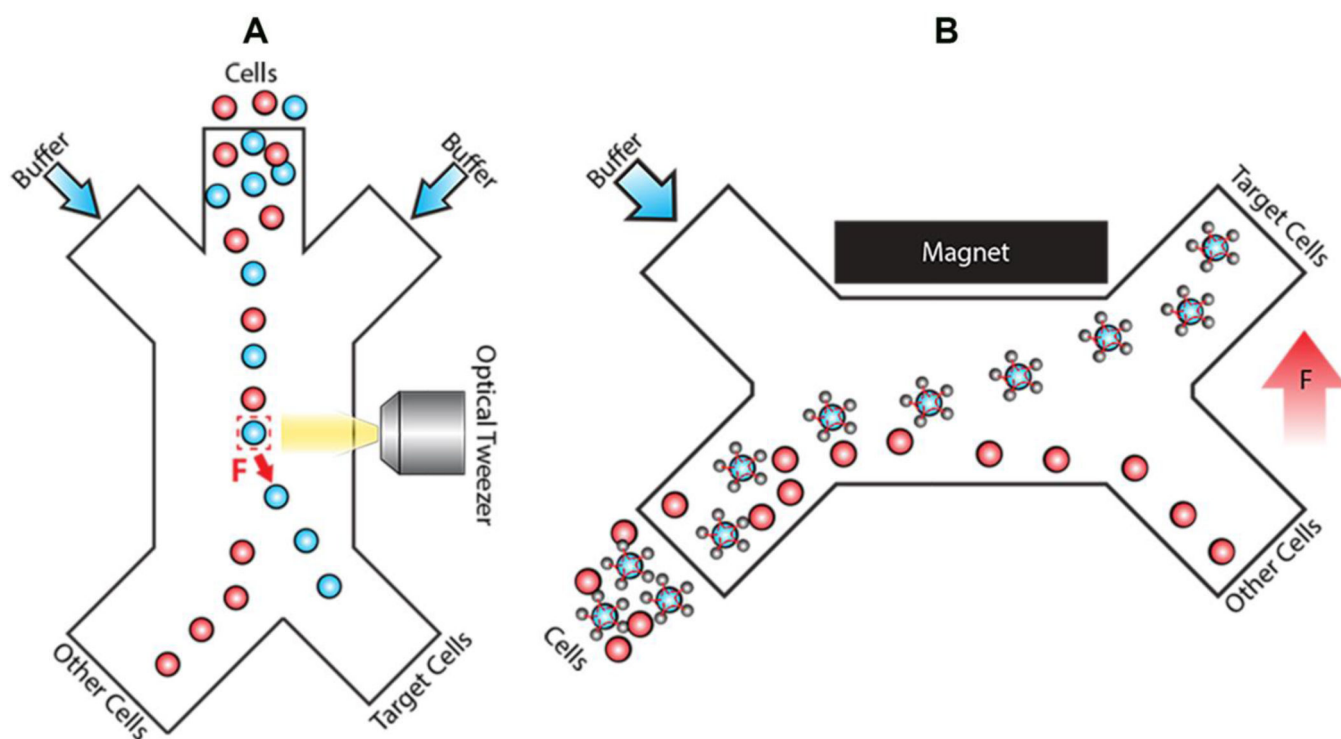


**Figure 6.**

Optical and magnetic based microscale cell separation techniques. (A) A schematic of optical cell separation. A laser grips onto cells traveling in focused flow via the “optical tweezer” effect and the cells are repositioned toward the appropriate outlet. (B) A schematic of magnetic cell separation. Target cells are labeled with cell specific, antibody conjugated, magnetic beads prior to the microfluidic device. The device is operated in the presence of a magnetic field and the labeled target cells exit at a distinct outlet while non-target cells exit at a separate device outlet.

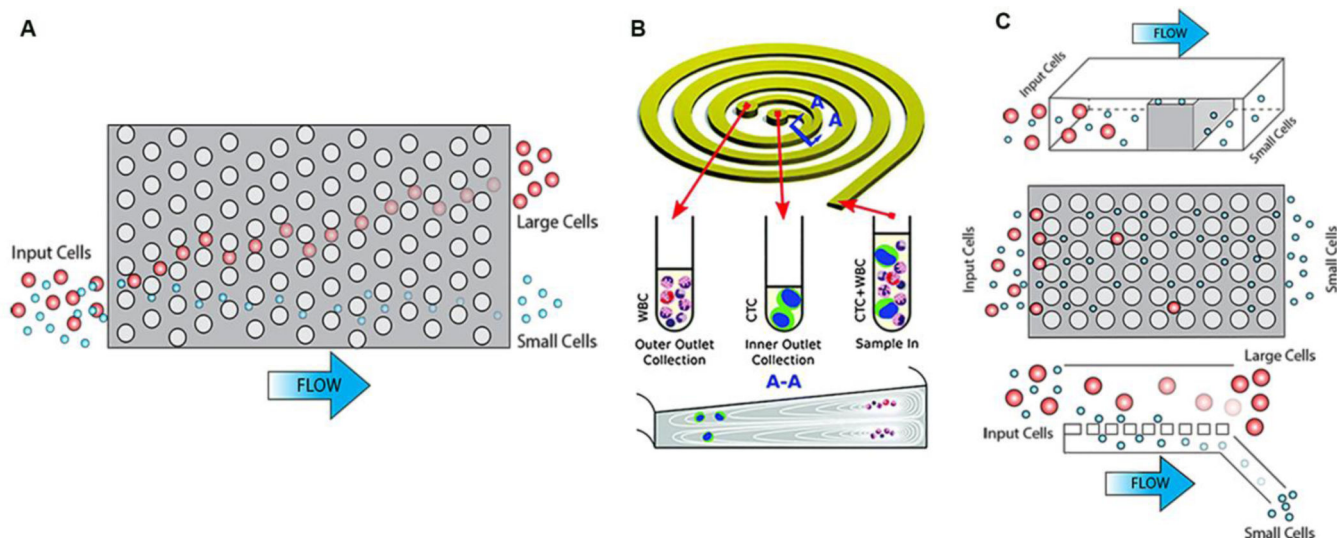


**Figure 7.** Passive microscale cell separation techniques. (A) A schematic diagram of DLD based cell separation. An array of pillars directs cells with a radius greater than the critical radius toward a distinct outlet. (B) A schematic diagram of inertial based cell separation in spiral microfluidics. The spiral channel design results in vortex formation perpendicular to the primary flow at two distinct regions, also known as Dean flow. Cells with different physical properties are focused at a particular vortex and the cells are separated via bifurcating outlets. Reproduced from Di Carlo, D. *Lab on a chip* 2009, 9 (21), 3038-46 (ref 101), with permission of the Royal Society of Chemistry. (C) A schematic diagram of filtration based cell separation, showing three filter configurations. From top to bottom: the weir filter, the pillar filter, and the cross-flow filter.

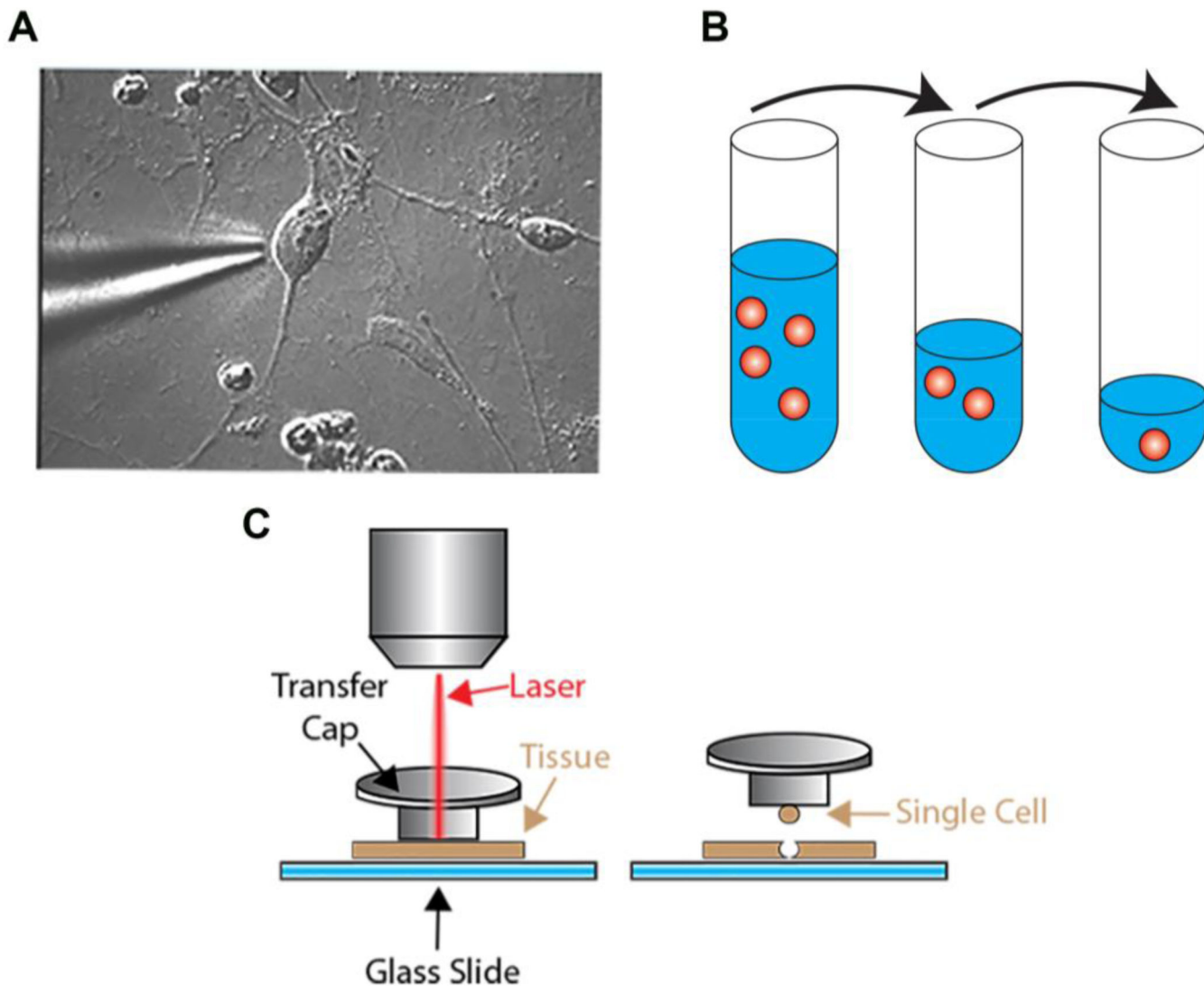


**Figure 8.**

Conventional single cell isolation techniques. (A) A microscopy image showing single neuron isolation via a micromanipulator and pipette. When the pipette contacts the single cell, a slight negative pressure sucks the cells into the pipette and the cell is transferred to a vessel for further processing. Reprinted by permission from Macmillan Publishers Ltd: Nature Protocols (ref 124), copyright 2011. (B) A schematic of single cell isolation via serial dilution. A cell suspension is diluted step-wise until only a single cell remains. (C) A schematic of single cell isolation via LCM. Tissue on a glass slide is positioned underneath an inverted microscope. A cap with a thermoplastic film bottom is placed on top of the tissue, with the film contacting the tissue. Once a target cell is identified, an infrared laser heats the thermoplastic film above the cell, thereby melting and adhering the film to the target cell. When the cap is removed, the adhered cell is selectively sheared from the tissue.

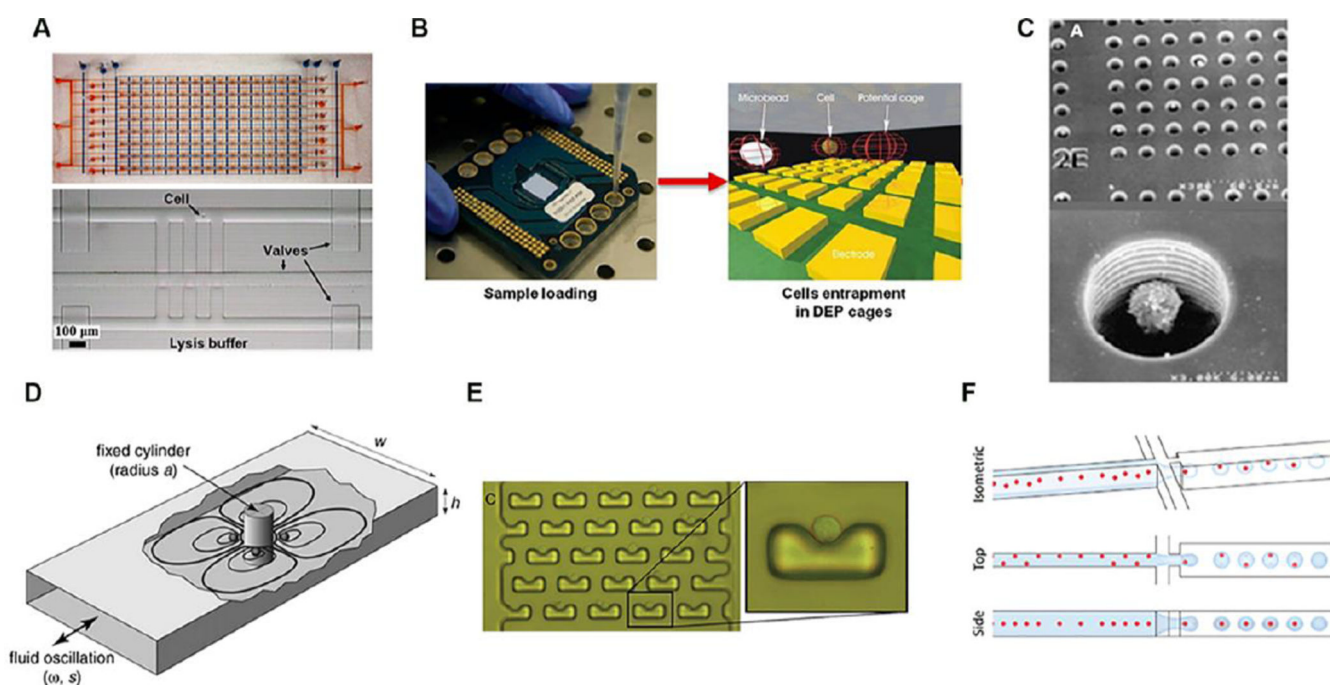


**Figure 9.**

Microscale single cell isolation techniques. (A) Quake valves for single cell isolation. Top photograph: an array of Quake valves. The channels with blue dye are pneumatic control channels and the channels with orange dye are fluid channels. Bottom microscope image: fluid and control channels intersect to form a chamber for single cell isolation. Reprinted with permission from Shi, Q.; Qin, L.; Wei, W.; Geng, F.; Fan, R.; Shin, Y. S.; Guo, D.; Hood, L.; Mischel, P. S.; Heath, J. R. *Proc Natl Acad Sci U S A* 2012, 109 (2), 419-24 (ref 141). Copyright 2011 Proceedings of the National Academy of Sciences of the United States of America. (B) Left photograph: the DEPArray™ chip. Right schematic: individually controlled electrodes on the chip bottom create DEP cages to trap single cells. Reprinted from *Cancer Letters*, Vol. 335, Fabbri, F.; Carloni, S.; Zoli, W.; Ulivi, P.; Gallerani, G.; Fici, P.; Chiadini, E.; Passardi, A.; Frassinetti, G. L.; Ragazzini, A.; Amadori. Detection and recovery of circulating colon cancer cells using a dielectrophoresis based device: KRAS mutation status in pure CTCs, pp. 225–231 (ref 144). Copyright 2013, with permission from Elsevier. (C) Top scanning electron micrograph: an array of wells for single cell isolation. Bottom scanning electron micrograph: a single cell confined inside of a single 10 μm diameter well. Reprinted from *Biochimica et Biophysica Acta*, Vol. 1810, Lindstrom, S.; Andersson-Svahn. Miniaturization of biological assays — Overview on microwell devices for single cell analyses, pp. 308–316 (ref 149). Copyright 2011, with permission from Elsevier. (D) A schematic of the “hydrodynamic tweezer” effect. An oscillating flow around a cylinder generates four recirculating eddies. Single cells are confined at the eddy center. Reproduced from Lutz, B. R.; Chen, J.; Schwartz, D. T. *Analytical chemistry* 2006, 78 (15), 5429–5435 (ref 152). Copyright 2013 American Chemical Society. (E) A microscopy image of single cell isolation via cup shaped physical traps. The inset shows a single cell seated at the trap. Reproduced from Di Carlo, D.; Wu, L. Y.; Lee, L. P. *Lab on a chip* 2006, 6 (11), 1445-9 (ref 157), with permission of the Royal Society of Chemistry. (F) A schematic

illustrating droplet based single cell isolation from isometric, top, and side viewpoints. Single cells in an aqueous buffer are introduced through the middle channel while immiscible fluid intersects the aqueous flow from two opposite channels perpendicular to the aqueous fluid flow. The result is an aqueous droplet containing a single cell. Reproduced from Edd, J. F.; Di Carlo, D.; Humphry, K. J.; Koster, S.; Irimia, D.; Weitz, D. A.; Toner, M. *Lab on a chip* 2008, 8 (8), 1262–1264 (ref 171), with permission of the Royal Society of Chemistry.



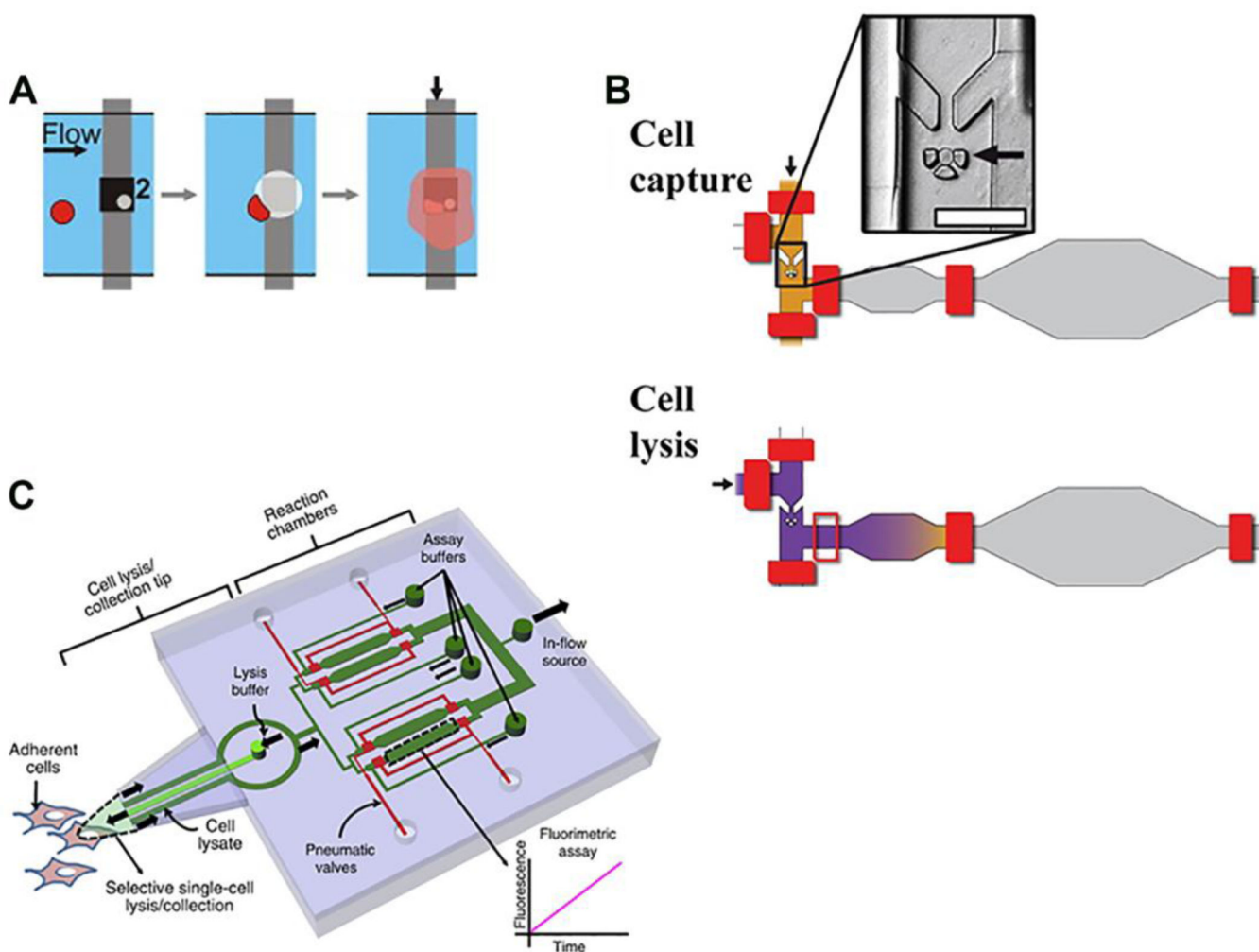


**Figure 10.** Microscale single cell lysis techniques. (A) A schematic illustrating mechanical single cell lysis. A channel of flowing fluid is heated via an integrated heater on the channel bottom, thereby generating a bubble above the heater. Single cells passing above the heater are lysed by the rising bubble. Reprinted from *Sensors and Actuators B: Chemical*, Vol. 168, Hoefemann, H.; Wadle, S.; Bakhtina, N.; Kondrashov, V.; Wangler, N.; Zengerle, R. *Sorting and lysis of single cells by BubbleJet technology*, pp. 442–445 (ref 191). Copyright 2012, with permission from Elsevier. (B) A schematic illustrating chemical single cell lysis. A single cell is trapped in chamber defined by flanking Quake valves. Post cell capture, lysis buffer is introduced into the chamber and the reagent is mixed via actuating Quake valves to facilitate lysis. Reproduced from White, A. K.; Heyries, K. A.; Doolin, C.; Vaninsberghe, M.; Hansen, C. L. *Analytical chemistry* 2013, 85 (15), 7182-90 (ref 8). Copyright 2013 American Chemical Society. (C) A schematic of a microfluidic device for single cell lysis in adherent cell culture. The device tip is positioned at the target cell and a hydrodynamically focused lysis buffer selectively lyses the single target cell. The single cell lysate is captured

on chip for fluorometric assay. Reprinted by permission from Macmillan Publishers Ltd:  
Nature Communications (ref 215), copyright 2014.

Author Manuscript

Author Manuscript

Author Manuscript

Author Manuscript